1990

Determination of manganese in seawater by flow injection analysis with chemiluminescence detection

Thomas P. Chapin
San Jose State University

Follow this and additional works at: https://scholarworks.sjsu.edu/etd_theses

INFORMATION TO USERS

The most advanced technology has been used to photograph and reproduce this manuscript from the microfilm master. UMI films the text directly from the original or copy submitted. Thus, some thesis and dissertation copies are in typewriter face, while others may be from any type of computer printer.

The quality of this reproduction is dependent upon the quality of the copy submitted. Broken or indistinct print, colored or poor quality illustrations and photographs, print bleedthrough, substandard margins, and improper alignment can adversely affect reproduction.

In the unlikely event that the author did not send UMI a complete manuscript and there are missing pages, these will be noted. Also, if unauthorized copyright material had to be removed, a note will indicate the deletion.

Oversize materials (e.g., maps, drawings, charts) are reproduced by sectioning the original, beginning at the upper left-hand corner and continuing from left to right in equal sections with small overlaps. Each original is also photographed in one exposure and is included in reduced form at the back of the book.

Photographs included in the original manuscript have been reproduced xerographically in this copy. Higher quality 6" x 9" black and white photographic prints are available for any photographs or illustrations appearing in this copy for an additional charge. Contact UMI directly to order.

Determination of manganese in seawater by flow injection
analysis with chemiluminescene detection

Chapin, Thomas Peterson, M.S.

San Jose State University, 1990

DETERMINATION OF MANGANESE IN SEAWATER BY FLOW INJECTION ANALYSIS WITH CHEMILUMINESCENCE DETECTION

A Thesis

Presented to

The Faculty of Moss Landing Marine Laboratories

In Partial Fulfillment

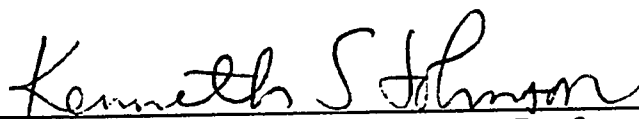of the Requirements for the Degree

Master of Sciences

in Marine Sciences

By

Thomas P. Chapin
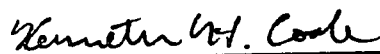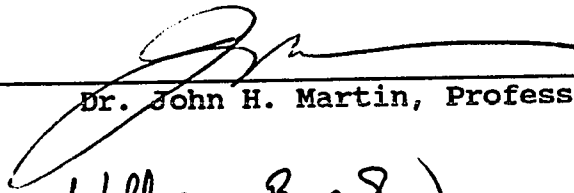
May 1990

APPROVED FOR MOSS LANDING MARINE LABORATORIES

_____
Dr. Kenneth S. Johnson, Professor
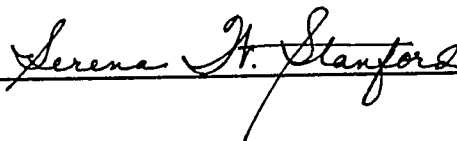

_____
Dr. Kenneth H. Coale

_____
Dr. John H. Martin, Professor

_____
Dr. William W. Broenkow, Professor

APPROVED FOR THE UNIVERSITY

_____

ABSTRACT

DETERMINATION OF MANGANESE IN SEAWATER BY FLOW INJECTION ANALYSIS WITH CHEMILUMINESCENCE DETECTION

by Thomas P. Chapin

Flow injection analysis (FIA) with chemiluminescence detection (CL) was used to determine manganese in seawater. The oxidation of 7,7,8,8- tetracyanoquinodimethane (TCNQ) in an alkaline solution emits light. Manganese (II) catalyzes this reaction and the concentration of Mn(II) can be determined by measuring the rate of photon emission. A column containing 8-hydroxyquinoline immobilized on a solid support was used in-line in the FIA system to concentrate Mn and separate it from the alkaline earth metals. Analysis time was 6 minutes per seawater sample with a corresponding detection limit of 0.1 nM. Lower detection limits can be obtained by extending the amount of time manganese is loaded onto the column. The average standard deviation of analyses of seawater containing 2 nM manganese was $\pm$ 3% (n=5). Shipboard analyses of Mn on the PS89 cruise at stations off the California coast produced excellent agreement with previous reliable Mn data (1, 2) and demonstrate the accuracy of the technique.

ACKNOWLEDGEMENTS

I wish to express my deepest gratitude to Dr. Ken Johnson, Dr. Kenneth Coale, Dr. William Broenkow, and Dr. John Martin for their constant support, guidance, and enthusiasm in this research. I would also like to thank Virginia Elrod, and Carol Chin of the Moss Landing Marine Labs Chemical Oceanography Group for the scientific and emotional support they provided. The excellent CTD operation on the Point Sur June 1989 cruise was performed by Andy Heard while Janie Berger and Nina Greenberg were the oxygen wizards. As usual, the operation of the RV Point Sur was flawless and I wish to express my gratitude to the captain and the crew.

This thesis was greatly enhanced by the rigorous and patient reviews of Drs. Johnson and Coale who have been a tremendously inspiring and valuable influence upon my life.

TABLE OF CONTENTS

LIST OF TABLES

LIST OF FIGURES

INTRODUCTION

Only within the last 15 years have reliable analytical techniques been developed that allow the determination of trace metals in seawater at low nanomolar to picomolar concentrations (3, 4, 5). Most of the reliable trace metal analyses that have been performed on seawater have used Graphite Furnace Atomic Absorption Spectrometry (GFAAS) after preconcentration of the sample (3, 4, 5). Analyses utilizing this method require complex instrumentation, laborious sample preparation, and clean laboratory facilities that are usually only available in shore based labs. This limits the number of determinations that can be made and it precludes a flexible sampling design. Simple, inexpensive methods of trace metal analysis must be developed if shipboard methods of analysis are to become widespread. Some progress has bee made through the use of electrochemical (6) and gas chromatographic techniques (7). Other methods must be developed to broaden the suite of metals that are amenable to near real-time analysis on board ship.

The goal of this work was to develop a rapid, sensitive, and portable method for the determination of Mn(II) in seawater. Manganese has been one of the most thoroughly studied trace metals in the sea (1, 2, 4, 8). However,

because of its unique biogeochemistry, Mn distributions in the ocean are very complicated. Many more analyses will be required to obtain a satisfactory understanding of the processes that control its distribution. A simple shipboard method for the analysis of manganese at sub-nanomolar levels is needed.

Yamada et al. (9) demonstrated that Mn(II) can be determined with a high sensitivity and selectivity based on the Mn catalysis of the oxidation of 7, 7, 8, 8-tetracyano-quinodimethane (TCNQ) and the subsequent production of chemiluminescence. This technique can be readily adapted to an automated analysis using flow injection analysis (FIA). As a result it requires very little sample handling or manipulation and this eliminates many of the stringent "clean" practices often necessary for standard manganese analysis. Flow injection analysis has proven to be a simple, robust method of analysis that is well suited for use onboard ship (10, 11, 12, 13).

In this thesis I will report the results of my work to adapt the Mn catalyzed oxidation of TCNQ for the determination of manganese in seawater and present results obtained on the Point Sur 1989 (PS89) cruise at stations off the California coast. I begin by reviewing the previous work that has been done to study the manganese biogeochemistry in the ocean.

MANGANESE BIOGEOCHEMISTRY

Manganese has become a very useful tracer of biogeochemical cycling in the marine environment. The relative ease of Mn oxidation and reduction results in its involvement in many biological and geological cycles. The processes affecting manganese distribution include atmospheric and fluvial input (14, 15); scavenging onto sinking particles (2, 8); photooxidation and reduction in surface waters (16, 17); microbiologically mediated redox processes (18, 19, 20, 21); advection/diffusion from sediments (1, 22, 23); and hydrothermal processes (24, 25). The interaction of these various processes controls the distribution of manganese in the marine environment. Figure 1 exhibits the major processes that control the distribution of manganese in seawater.

Speciation

Manganese can exist in three oxidation states under oceanic conditions: Mn(II), Mn(III), and Mn(IV). Thermodynamic calculations suggest that the oxides of the Mn(IV) state will predominate in oxic seawater (26). At a pH of 8.0, the predicted concentrations of Mn(III) and Mn(IV) are approximately 30 orders of magnitude greater than the concentration of Mn(II) (Fig. 2). The Mn(IV) oxidation state

is believed to occur as a variety of oxide phases or incorporated into alumino-silicates (15). These oxides should be rapidly removed from the dissolved phase due to their very low solubility. The Mn(III) oxidation state is thermodynamically unstable under oxic seawater conditions but it may exist as the metastable oxyhydroxide, MnOOH (27). These manganese oxyhydroxides may be an important intermediate phase in the oxidation of Mn(II) to Mn(IV) via chemical or biological processes (27). Manganese (II) is soluble in seawater. However, thermodynamic calculations suggest that Mn(II) should exist at subnanomlar concentrations in oxygenated seawater because of its tendency to oxidize to Mn(IV) (5, 15, 24).

The concentration of dissolved manganese, that fraction passing through a 0.45 μm filter, ranges from a low of 0.08 nM to levels over 10 nM under oceanic conditions (15). The dissolved fraction is often assumed to be Mn(II) although there is no direct evidence of this (15). Hydrothermal outputs of dissolved manganese can be on the order of 10-1000 nM or higher (24, 25). Since the observed concentrations are usually several orders of magnitude higher than would be predicted by thermodynamic calculations, the distribution of Mn in the ocean is probably controlled by a variety of kinetic processes. If this is indeed the case, then the observed concentrations represent a balance between the rates of input

and output. Efforts to understand the manganese distribution must focus on the processes that add and remove Mn from the ocean.

The inputs of manganese to the marine environment include eolian, fluvial, and hydrothermal fluxes, as well as diffusion from nearshore and pelagic sediments. The removal processes consist of adsorption and/or precipitation onto sinking particles, incorporation into organisms, and precipitation at the sediment/water interface (24). Each of these sources and sinks has a characteristic influence on the distribution of Mn in the sea. A sufficient number of measurements will allow us to resolve and study each of these processes.

The previous measurements of manganese distributions in the ocean reveal large changes in concentration in both the vertical and horizontal dimensions (1, 2, 5). The general vertical profile consists of a surface maxima, a subsurface minima usually below the mixed layer, midwater maxima associated with the oxygen minimum, and a relatively constant low deep water concentrations with an increase just above the sediments. A second surface maxima just below the mixed layer has frequently been observed but does not appear to be a constant or universal feature (1). Manganese profiles in the Pacific and Atlantic share the same general characteristics but the Atlantic concentrations are higher (28). This can be attributed to the increase in riverine and atmospheric input

to the Atlantic and the deep water circulation patterns. The older Pacific deep water has had more time for the manganese to be scavenged away, resulting in lower deep water values. The general manganese profile differs markedly from the "nutrient-like" profiles of trace metals such as Cd, Zn, Cr, and Ni, or the "surface depletion, depletion at depth" trace metals such as Fe and Cr (15).

Previous studies of manganese geochemistry have relied on a variety of schemes to determine the speciation of Mn in an effort to elucidate the processes that control its concentration. One limitation of many of these speciation studies is an inability to differentiate the various oxidation states of Mn at nanomolar concentrations. Consequently many operational definitions have come into use. Bender et al. (26) acidified their unfiltered samples to pH 2 and analyzed for "total dissolvable Mn," (TDM). Martin and Knauer (1, 22, 23) and Landing and Bruland (2, 5) separated the manganese into dissolved and particulate fractions by filtering seawater through polycarbonate membrane filters (0.45 μm pore size). In addition, they divided the particulate manganese fraction into "weak acid leachable" manganese (HAc), and refractory manganese (REF) by performing selective leach experiments on the filtered particulate samples (29, 30). Weak acid leachable manganese was that fraction which was desorbed from the particles upon treatment with a 25% acetic acid solution.

Refractory manganese was the particulate material remaining after the weak acid leach. This material was subjected to digestion with concentrated HCl, HNO_3, and HF and the resulting digest was analyzed.

Weak acid leachable manganese was believed to be the fraction that was weakly adsorbed onto particles, bound to Ca and Mg carbonates, skeletal matrices, and some fraction of the Mn oxyhydroxides (2). The refractory manganese was thought to be the manganese in the +4 oxidation state, presumably MnO_2, and insoluble manganese trapped in alumino-silicate mineral phases. According to Landing and Bruland (2), the ratio of acetic acid leachable (HAc) to refractory (REF) manganese should give an indication of the amount of dissolved manganese being adsorbed onto particles. High HAc:REF ratios would imply an increase in manganese scavenging while low HAc:REF ratios would identify areas where Mn oxyhydroxides were dissolving or increased alumino-silicate input predominated (2). Sunda and Huntsman (16) have refined the leaching process to distinguish between particulate manganese oxyhydroxides and adsorbed Mn. They compared the amount of dissolved Mn in a natural sample to one treated with 0.3 mM ascorbate. This mild ascorbate reduction at pH 8 solubilized the Mn oxyhydroxides while leaving the adsorbed Mn and iron oxyhydroxides intact.

These analytical tools have been employed to demonstrate

the existence of a number of characteristic features of the Mn distribution, and to infer from these distributions the processes that control the Mn concentrations. However, as is discussed below, these interpretations are often at odds. Much of this difficulty in interpretation is a consequence of the undersampling that results from the laborious analytical procedures that have been used previously to determine manganese in seawater.

Surface Manganese

The manganese surface maxima has been attributed to three processes; fluvial input, eolian input and diffusion from shelf sediments (5, 15, 26). Klinkhammer and Bender (8) proposed that atmospheric input was the dominant factor. Statham and Chester (14) demonstrated that manganese in the source material for eolian input to the oceans existed in the +4 oxidation state. However, this source material may be reduced while in the atmosphere by acid rain nuclei and also by photoreduction and could therefore enter the marine system in the +2 oxidation state. As much as 25% of the Mn in atmospheric particles was observed to rapidly dissolve (14). On the other hand, Landing and Bruland (5) found an inverse relationship between ^{210}Pb and manganese in the Pacific. Since the atmosphere is the major source of ^{210}Pb, they concluded that river input and shelf sediment input were more important

factors than atmospheric input near ocean boundaries.

The surface maxima must be maintained by a continuous input of manganese. Otherwise the removal of Mn due to the uptake of Mn by phytoplankton and scavenging onto sinking particles would erode the surface maxima. Manganese is required by plankton in a Mn:C molar ratio of approximately $10^{-6}:1$ (31). The manganese is used in photosynthesis to split water molecules in photo system II to form molecular oxygen, protons, and electrons. In addition, superoxide dismutase, a Mn based enzyme, detoxifies the superoxide radicals which are produced at elevated rates by photosynthesizing cells (17). There is also some evidence that suggests that Mn may be limiting production in the surface waters of the sub Arctic Pacific (32). For a coastal photosynthesis rate of 1000 mg C m^{-2} d^{-1} (33) and a 50 m euphotic zone, the surface manganese maximum of 2 nM Mn would be removed in 200 days.

Scavenging also removes manganese from the surface layer. Particles sink continuously from the surface, and any Mn adsorbed on to the surfaces of these particles will be removed as well. The adsorption step is often accompanied by oxidation of the manganese (19). Most metals are depleted in the surface waters by scavenging and increase with depth when the scavenging particles are remineralized. However, Mn retains its surface maxima in contrast to most other metals. Clearly, other processes are affecting the Mn distribution.

One of the processes that may act to reduce the significance of Mn scavenging in the euphotic zone is photochemical reduction. Sunda et al. (16, 17) have observed that Mn (IV) was reduced photochemically in surface waters. Particulate Mn was reduced to dissolved Mn by organic compounds commonly found in seawater such as humic and fulvic acids. The reducing power of these organic substances is enhanced by sunlight. Observations in the Sargasso Sea show a strong depletion in particulate manganese oxide concentrations near the surface (16).

Sunda and Huntsman (16) also demonstrated that bacteria were responsible for the formation of particulate Mn below the photic zone. In addition, their experiments demonstrated that these microbes were photoinhibited and were not able to oxidize Mn(II) in the photic zone. Photoinhibition of manganese oxidizing bacteria along with the photodissolution of particulate Mn would help to maintain the surface maxima in dissolved manganese (16). Photoinhibition of manganese oxidizing bacteria would decrease the formation and subsequent export of particulate Mn in the near surface waters. At the base of the mixed layer, the low light levels would no longer enhance photoreduction of oxidized manganese species and the bacteria would no longer be photoinhibited. Thus, dissolved manganese uptake by bacteria and particle formation can proceed. The increased rate of removal at low light

intensities probably accounts for the dissolved manganese minimum below the euphotic zone.

Manganese in the Oxygen Minimum

The manganese maxima associated with the oxygen minima is one of the most perplexing features of the Mn profile. Processes that might contribute to the maxima are: 1) oxidation of sinking organic material with the concomitant release of dissolved Mn; 2) desorption of Mn from particles; 3) reduction of manganese dioxide particle phases; 4) horizontal advection from coastal sources; and 5) decreases in the scavenging rate of Mn in this region. Under suboxic or anoxic conditions particulate manganese dioxide (IV) can be reduced to manganese(II) where it accumulates in the dissolved phase. This is a common feature of redox boundaries in the sediments and in stagnant basins such as the Black Sea (19). Reduction in the water column under anoxic conditions may contribute locally to the dissolved manganese maxima but the typical pE and pH values of oceanic water generally prevent the reduction of Mn(IV) to Mn(II). Landing and Bruland (2) attributed the Mn maxima to organic carbon regeneration and reduction of oxyhydroxides. Martin et al. (1) state that their finding of a constant organic flux through the oxygen minimum implies that no regeneration is taking place and therefore the Mn maxima can only be the result of horizontal

advection. Johnson (34) developed a numerical model that allowed for both regeneration of organic carbon, changes in the scavenging rate, and horizontal advection from continental sources. This model demonstrated very good agreement with the observed data. The manganese maxima associated with the oxygen minima is probably a result of all these different processes. Local conditions will determine which process will dominate in a given system.

Hydrothermal and Deep Water Manganese

Hydrothermal input appears to be the largest single source of dissolved manganese to the marine environment (5, 15). Manganese concentrations in hydrothermal fluid reach upwards of 1000 μM, a level one million times greater than the average seawater Mn concentration. However, even with this tremendous input, a dissolved Mn maxima corresponding to hydrothermal input is not an ocean wide feature but is isolated to within two thousand kilometers or less of ridge axes (25). The dissolved manganese from the vents interacts with the ambient deep seawater forming oxide particles that are deposited on the flanks of the ridge. The time scale of this oxidation is relatively fast with a residence time on the order of 50 years or less and this prevents the occurrence of an ocean wide manganese maxima corresponding to hydrothermal input (5, 25). The ratio of dissolved to particulate

manganese should increase as the water mass is advected away from the ridge axis and this ratio could be useful in tracing hydrothermal water mass movement and estimating velocities.

Deep water manganese values are generally the lowest and reflect the ongoing scavenging and removal from the water column (11). Near bottom Mn is elevated due to resuspension of the bottom sediments (15).

Particulate Manganese

Particulate manganese profiles display consistent features. Landing and Bruland (2) demonstrated: 1) refractory (REF) manganese near surface minima, consistent with incorporation into sinking particles via biological or adsorption processes; 2) subsurface REF maxima for stations near the North American coast resulting from horizontal advection of resuspended shelf sediments; 3) midwater maxima, 300-1200 m, probably also due to horizontal advection; and 4) and near bottom maxima caused by resuspension of bottom sediments. The levels of particulate Mn vary from approximately 1% of the total manganese at the surface to over 30% at depths of 100-750 m (5, 16). Landing and Bruland (2) reported that high HAc:REF ratios were observed immediately below the photic zone and this indicated that scavenging of Mn(II) onto particles was occurring. Sunda and Huntsman's ascorbate treatment solubilized Mn oxyhydroxides but not

adsorbed Mn(II) and they found that the particulate Mn immediately below the photic zone was almost all from the ascorbate labile fraction (16). Sunda and Huntsman (12) contend that the HAc fraction determined by Landing and Bruland (2, 5) and Martin and Knauer (1, 22, 23) was probably Mn oxyhydroxides and not manganese that had been adsorbed onto particles. Sunda (16, 17) proposes that these Mn oxyhydroxides are primarily produced by microbial oxidation and that this oxidation takes place extracellularly and the oxides are deposited on acidic polymers surrounding the bacteria. This result is supported by the findings of Cowen and Silver (20) and Cowen and Bruland (21) who reported high levels of manganese and iron associated with bacterial capsules. These bacterial capsules were often completely covered with iron and manganese containing "filaments" that greatly increased the surface area of the capsule.

Bacterial Transformation of Manganese

Evidence for the role of microorganisms in the oxidation, reduction, and scavenging of manganese in seawater is rapidly accumulating (18, 19, 20, 21). Some bacteria oxidize Mn(II) to produce particulate manganese oxyhydroxides with a mixed valence oxidation state of +2 to +3 (15). Grill (27) proposed a bacterially mediated two step process for the oxidation of Mn(II) to Mn(IV). The first step is the fast uptake of Mn(II)

by the bacteria followed by a slow oxidation. Grill (27) found an average oxidation state of +3.05 for particulate manganese in the Saanich inlet while Emerson et al. (19) found an average oxidation state of 2.3-2.7. These particulates probably exist as the oxyhydroxides and the maximum in particulate manganese is associated with a maximum in bacterial cell abundance. Emerson also demonstrated that the particulate formation was severely inhibited by biological poisons confirming that the manganese oxidation is bacterially mediated in the Saanich inlet system (19). Diem and Stumm (35) demonstrated that the oxidation of Mn(II) in sterile seawater did not occur even with a seven year long experiment. Sunda and Huntsman (16) found that bacteria were responsible for the formation of particulate Mn below the photic zone. Their experiments also demonstrated that these microbes were photoinhibited and were not able to oxidize Mn(II) in the photic zone. Cowen et al. (36) established that bacteria were involved in the oxidation of dissolved manganese released from hydrothermal vents along the Juan de Fuca Ridge.

Manganese is also utilized by some anaerobic bacteria as the terminal electron receptor in the oxidation of organic material. These bacteria reduce particulate Mn(IV) to Mn(II), which is soluble (18). The anoxic conditions required for this process are usually well below the sediment water interface. The oxygenated sediments near the sediment-water

interface in most pelagic regions effectively "cap" the diffusion of reduced manganese out of the sediments. Aerobic bacteria reoxidize the reduced manganese as it diffuses into oxygenated sediments where it forms a layer of Mn rich particles. Consequently most oxygenated sediments are not thought to be a major source of dissolved manganese (5). However, due to the high productivity of coastal areas, sediments along the continental shelf and slope are often organic rich. The high organic load can deplete the oxygen in the water column and create suboxic or anoxic conditions at the sediment-water interface along the shelf and slope sediments. These sediments may be a large source of Mn (1, 5, 26). The dissolved manganese can then be advected horizontally away from the coast creating a midwater Mn maxima that coincides with the oxygen minimum (1, 2).

Manganese is a powerful tracer of many oceanic processes including horizontal advection from nearshore sediments and hydrothermal systems, oxic/anoxic interfaces, offshore jets and plumes, scavenging processes, and regeneration and microbial interaction.

In light of the escalating costs of ship time, there is a demand for new analytical techniques. These techniques should be sensitive, noncontaminating, inexpensive, portable, rapid, and reliable. Reported here is the development of a new technique for the analysis of manganese in seawater based

on the Mn catalyzed oxidation of TCNQ with chemiluminescence detection that satisfies these requirements.

FLOW INJECTION ANALYSIS AND CHEMILUMINESCENCE

Since its development in the mid 1970's, flow injection analysis (FIA) has become a widely adopted technique for automated chemical analysis (37). The technique is based on mixing a slug of sample with a continuous, unsegmented stream of reagents in a capillary tube. This allows the accurate and very reproducible mixing of reagents and sample and delivery to a flow through detector. Reproducible mixing and timing allow one to perform many analyses without waiting for the reaction to achieve equilibrium. Reagent and sample handling are reduced to a minimum since a peristaltic pump is used to introduce, transport, and mix solutions within the system. The sample and reagent volumes that are used in a typical FIA system are low with flow rates on the order of 1-2 ml/min.

Initially FIA was used to automate and simplify the chemical analysis of compounds present at relatively high concentrations such as the nutrient analysis of phosphate and nitrate. Detectors with relatively low sensitivity such as spectrophotometers and electrochemical detectors based on potentiometry and amperometry were used for this work. Recently FIA has been applied to trace metal analysis. This

has required the development of more sensitive detectors based on a variety of techniques including inductively coupled plasma mass spectrometry, anodic stripping voltametry, and chemiluminescence (9, 38, 39, 40, 41, 42).

Chemiluminescence in conjunction with flow injection analysis is gaining wide acceptance for trace metal analysis (9, 38, 39, 40). The detection technique is very sensitive and the instrumentation is simple and inexpensive. The usual underlying principle is the oxidation of a highly conjugated organic molecule creating an excited product which emits photons as it decays to the ground state. In most reaction systems either singlet molecular oxygen or excited organic molecules resulting from the energy transfer from the singlet molecular oxygen are the actual photon emitters (39). Trace metals can catalyze or enhance some of these reactions and increase the rate of the photon emission. Trace metal analysis can exploit this principle when reactions which are highly specific to a given metal can be identified. A number of techniques have been developed that have the necessary high degree of catalyst or enhancer specificity and these techniques have been adapted to analyzing metal at trace concentrations (9, 38, 39, 40).

Fedorova et al. (43) demonstrated that the oxidation of 7, 7, 8, 8-tetracyanoquinodimethane (TCNQ) has a very high chemiluminescence efficiency. Yamada et al. studied the

mechanism of the reaction and found that manganese behaved as a catalyst for the oxidation of TCNQ (9). They further showed that a surfactant, didodecyldimethylammonium bromide (DDAB) can be used to solubilize the TCNQ and increase the rate of reaction by allowing a more efficient transfer of energy to the luminescing reagent. DDAB has two long alkyl chains and these create a bilayer aggregate and not a micelle as used in other systems (38, 39, 40). The charged ammonium region of DDAB creates a hydrophilic exterior while the alkyl chains produce a hydrophobic interior which can solubilize the TCNQ (44). The higher organization and stability of the bilayer also allows for a more effective transfer of energy to the sensitizer, in this case Eosin-Y.

TCNQ is a very strong electron receptor due to the cumulative electron withdrawal of the four cyano groups. The addition of the DDAB creates a charge transfer complex with TCNQ. Yamada et al. (9) proposed that the reaction mechanism for the observed background chemiluminescence would proceed with the alkaline hydrolysis of TCNQ to create dicyano-p-toluoylcyanide (DCTC$^-$) which then reacts with the dissolved oxygen to emit photons. The Mn (II) catalysis proceeds by an unknown mechanism, but it is plausible that the TCNQ anion radical, created by the solubilization of TCNQ in DDAB, catalytically reacts with the manganese to produce an unknown compound which emits photons. This reaction scheme is

illustrated in Figure 3. Yamada et al. (9) was able to confirm the catalytic effect of Mn (II) by demonstrating that changes in the absorption spectra of both the DCTC⁻ ion and the unknown compound depended upon the manganese concentration. Increasing the manganese concentration decreased the DCTC⁻ ion absorption band at 470 nm while increasing the absorption band of the unknown compound at 345 nm (9). The resulting system permits manganese to be determined at nanomolar concentrations with fewer interferents than most chemiluminescence systems.

EXPERIMENTAL SECTION

A schematic diagram of the FIA manifold used for the determination of manganese is shown in Figure 4. The sample and reagents were pumped with a Gilson Minipuls 2 eight channel peristaltic pump. Fisher blue/yellow tygon tubing (1.52 mm I.D.) was used for the sample and HCl elution channels. Initially, the NaOH and luminescing reagent (R1) pump tubing lines were also 1.52 mm I.D.. In an effort to reduce reagent consumption, the NaOH and R1 lines were later changed to Fischer white/white tygon tubing (0.7 mm I.D.). At a pump setting of 600, this produced a flow rate of 2.7 ml/min for the blue/yellow tygon tubing and 1.3 ml/min for the white/white tygon tubing. All other manifold lines consisted of 0.8 mm I.D. teflon tubing except for a 0.5 mm I.D. teflon

line from the injection valve to the reaction flow cell. This line decreased the time required to inject the sample into the luminescing reagents and resulted in higher sensitivity. A multiport stream selection valve, V1, was used to control the sequence of solutions that flowed through the inlet port of the rotary injection valve, V2, and then through a column of immobilized 8-hydroxyquinoline (8-HQ) (38) that was placed in the sample loop of V2. The solutions pumped through valve V1 were used to wash, load, and rinse the 8-HQ column while valve V2 was used to elute the Mn from the 8-HQ column and inject it into the reaction flow cell. The position of the valves were controlled by a Compaq microcomputer equipped with a Metrabyte Dascon-1 A/D converter and digital interface.

The analytical cycle consisted of a 4 minute sample load onto the 8-HQ column, a 1 minute Milli-Q (MQ) column rinse to remove the alkaline earth metals, followed by a 0.75 minute elution/detection period using 0.0025 M HCl. Finally a 0.25 minute strong acid (1.0 M HCl/ 0.1 M HNO_3) wash completely removes any residual metals after the elution/detection period.

The chemiluminescence is almost instantaneous so the Mn sample is mixed with the TCNQ/NaOH solution in the flow cell mounted directly in front of the photomultiplier tube (PMT). The flow cell consists of a 25 cm length of 1.27 mm I.D. clear tygon tubing coiled into a PVC holder that is O-ring sealed

and screws onto a Pacific Instruments Model 3547 PMT housing.
A Hamatsu R268 photomultiplier tube was cooled to
approximately -15° C with a Pacific Instruments 33 Cooler
which reduced the baseline noise by over 500 counts sec^{-1}. The
photomultiplier output signal was amplified by a Pacific
Instruments Model 126 photometer. Data was recorded both with
a strip chart recorder, and by the microcomputer. Figure 5
displays a typical chart recorder output for the standard
addition of manganese to seawater.

Fresh seawater samples are analyzed at natural pH without
any manipulation. Particulate matter can clog the 8-HQ column
which leads to erratic results. Therefore, surface samples
with a high particulate concentration should be filtered prior
to analysis. Consequently, acid washed 25 mm diameter 0.45 μm
poresize teflon membrane filters can be used in line to filter
surface samples. A manually operated multiport valve was
positioned between the stream selection valve, V1, and the 8-
HQ column. This arrangement allowed the filter to be added to
the flow scheme for surface samples by rotating the valve
(Fig. 4). When in use the filter was acid washed and rinsed
with every cycle and dissolved Mn was measured. If the sample
was acidified for storage, it was adjusted to a pH 8 with
Ultrex ammonium hydroxide prior to analysis. If the sample
was not filtered prior to acidification, then total
dissolvable manganese (TDM) was determined. This system was

automated with the addition of a Isco Isis autosampler which greatly reduced the sample handling and permitted other FIA-CL systems to analyze the same sample.

Reagents

Ultrapure chemicals were not strictly required because any manganese contamination in the reagents was accounted for in the background chemiluminescence. High purity TCNQ, DDAB, and Eosin-Y and reagent grade HCl and NaOH were used for the analyses. However, if samples were acidified with HCl for storage and then adjusted to pH 8 with NH_4OH prior to analysis, ultrapure HCl and NH_4OH were used to decrease the reagent blank. The 7, 7, 8, 8- tetracyanoquinodimethane (TCNQ), and didodecyldimethylammonium bromide (DDAB) were obtained from Kodak. The Eosin-Y, reagent grade sodium hydroxide, reagent grade HCl, reagent grade HNO_3, and Ultrex ammonium hydroxide were from Fisher. Double distilled 6 M HCl from GFS Chemicals was used as received. No significant difference in sensitivity or background emission was observed when reagent grade HCl was replaced with high purity GFS 6 M HCl. Replacing the sodium hydroxide with Fisher Ultrex NH_4OH actually resulted in a decrease in sensitivity perhaps due to an interference effect from the ammonium ion.

The reagents were made up in 18 Mohm cm^{-1} Millipore Milli-Q water (MQ water). All glassware and plastic ware was

cleaned by soaking 24 hours in 10% Micro detergent followed by 24 hours in a 1 M HCl bath. After the initial cleaning, the glass and plastic ware was stored with 10% HCl and rinsed with MQ water prior to use. Besides the sample, only the MQ rinse and the column acid wash went through the 8-HQ column. Since the acid wash was too acidic to allow any manganese to remain on the column, the only source of contamination was in the MQ rinse and this was easily controlled by running MQ blanks during the analysis to check for contamination.

Reagents and Standards Preparation

Reagent R1: 5.0 ml of 0.06 M Eosin-Y solution was added to 900 ml MQ water. 0.01 g TCNQ and 1.85 g DDAB were added and the mixture was brought up to 1000 ml with MQ water. Shake occasionally and sonicate in a Branson B-22-4 ultrasonic bath for one hour. The sonication helped to solubilize the TCNQ. The final concentration was 5×10^{-5} M TCNQ, 4×10^{-3} M DDAB, and 3×10^{-4} M Eosin-Y. The working solution was usually stable for 12 hours.

1 M HCl/0.1 M HNO$_3$: 86 ml conc. HCl (Fisher reagent grade) and 6.5 ml of conc. HNO$_3$ (Fisher reagent grade) were diluted to 1000 ml.

0.0025 M HCl: 10 ml of 0.25 M HCl was diluted to 1000 ml. This reagent was prepared daily.

0.01 M NaOH: 20 ml of 0.5 M NaOH was diluted to 1000 ml.

This reagent was prepared daily.

Standards: 50 μM and 1μM Mn stock solutions were made up from a 1000 ppm Mn standard (Fisher) diluted with MQ water and acidified with 25 μL 6 M GFS HCL per 100 ml of standard Stock solutions were prepared monthly. Working standards were prepared daily by dilution of these stock solutions.

RESULTS AND DISCUSSION

We initially attempted to analyze Mn in seawater using the single valve manifold described by Yamada et al. (9). However, this system lacked sufficient sensitivity for the direct determination of Mn at concentrations less than 20 nM. We, therefore, focused our efforts on a system that incorporated a column of an immobilized ion exchanger (45) to concentrate the Mn. This resulted in a large increase in sensitivity.

Optimization of reaction conditions

The concentrations of TCNQ, Eosin-Y, DDAB, sodium hydroxide, and hydrochloric acid were all optimized with the FIA system for standards in MQ water and seawater. In general, the concentrations of the reagents were kept to a minimum in order to reduce the background chemiluminescence and reagent blanks while still maintaining adequate

sensitivity.

The concentrations of TCNQ, DDAB, and Eosin-Y were not as critical as for the other reagents as long as threshold levels were reached. The optimum reagent concentrations were 5×10^{-5} M TCNQ, 4×10^{-3} M DDAB, and 3×10^{-4} M Eosin-Y, all values very similar to the results obtained by Yamada et al. (9). Higher concentrations of TCNQ, DDAB, and Eosin-Y usually resulted in increased background chemiluminescence without any significant increase in sensitivity (Figs. 6, 7, 8). Initially, the R1 mixture was pumped at a rate of 2.7 ml/min. In order to reduce reagent consumption, the flow rate was later decreased to 1.3 ml/min (the NaOH flow rate was also reduced), and this flow rate reduced background emission while maintaining sensitivity. A minimum of 30 minutes of sonification of the R1 reagent was required to ensure complete solubilization of the TCNQ within the DDAB/Eosin-Y solution. The TCNQ was added dry for the preparation of the R1 reagent because attempts to create a stock concentrated TCNQ solution were not successful. The R1 solution was usually stable for a 12 hour period but occasionally a rapidly rising or falling baseline or a high background chemiluminescence would indicate an unstable solution. The cause for this instability has not yet been isolated but appears to be related to the specific batch of reagents used and the containers in which the R1 solution was made.

The ideal reaction conditions within in the flow cell required a pH over 11 (Fig. 9). Variations in reaction pH could shift the baseline and produce spurious signals. Changes in pH may have resulted from the large change in proton concentration that occurs when the small volume of MQ water (pH~6) that filled the 8-HQ column at the time valve V2 was introduced into the HCl carrier stream. This MQ water slug would have produced higher pH values when mixed with the R1/NaOH stream. The injection spike associated with this large pH change caused a baseline shift that can obscure small signals due to Mn. The key to optimizing the HCl and NaOH levels was to use the weakest possible acid to elute the column and to use just enough NaOH to reach a pH greater than 11 within the flow cell. The best results were obtained with an NaOH:HCl molar concentration ratio between 1:1 and 2:1 (Fig. 9). A more acidic ratio led to a significant suppression of the background chemiluminescence and larger injection spikes while a more alkaline ratio resulted in a higher background without any gain in sensitivity (Fig. 9). For the given TCNQ, DDAB, and Eosin-Y concentrations and flow rates, a minimum level of 0.005 M NaOH was necessary for sufficient chemiluminescence (Fig. 10). Initially, the NaOH reagent was pumped at a rate of 2.7 ml/min and a concentration of 0.005 M. To reduce reagent consumption, the NaOH concentration was doubled to 0.01 M while the flow rate was

halved to 1.3 ml/min, and this still maintained the optimum NaOH concentration. The 8-HQ column required a minimum HCl concentration of 0.002 M (pH < 3) to quantitatively and reproducibly elute the manganese (Fig. 11). Consequently, 0.01 M NaOH and 0.0025 M HCl were chosen to ensure efficient elution and chemiluminescence and to minimize the large background or injection spikes caused by higher levels of these reagents.

After the R1 solution and NaOH reagent mix, the resulting solution is pumped into the flow cell in front of the PMT and mixed with the sample (Fig. 4). The amount of mixing that the R1 and NaOH undergo prior to the injection of the manganese sample was also critical. Too little mixing resulted in higher background chemiluminescence and increased baseline noise probably due to insufficient reagent mixing. Too much mixing allowed for more complete oxidation of the TCNQ before it reacted with the manganese and consequently reduced sensitivity (Fig. 12).

8-hydroxyquinoline columns (8-HQ)

The immobilized 8-HQ resin was prepared following the technique of Landing et al. (45). The resin was loosely packed into a column 1-1.5 cm long and 3.0 mm I.D. These columns proved to be extremely stable and reproducible and columns could be used for months at a time. Relatively high

flow rates were required to load sufficient Mn onto the column in the shortest possible time. This necessitated a large 3.0 mm I.D. teflon preconcentration column to eliminate any back pressure problems. These columns were jam fitted over the 0.8 mm I.D. injection loop tubing and this created a leakproof seal that allowed for rapid column changing (Fig. 4). Eventually the 0.8 mm I.D. sample loop tubing would compress and need replacement. The larger volume of the column also allowed for the use of more 8-HQ resin which greatly improved the efficiency of the extraction of the manganese from seawater. In addition to concentrating the manganese, the 8-HQ column also served to separate the Mn from the alkaline earth metals, which can interfere with the chemiluminescence reaction.

The pH of the sample had to fall within a limited range in order for Mn to bind to the 8-HQ column (Fig. 13). Fortunately, unacidified seawater samples, with a pH range of 7.5-8.5, are within this optimum range and this greatly simplified sample handling. After the sample was loaded onto the column, a 1 minute rinse (~3 ml) with MQ water effectively removed the alkaline earth metals from the column. Longer column rinse times run the possible risk of increasing the blank due to Mn contamination from the MQ water. The pH of the MQ rinse was critical since a lower pH solution would elute the manganese from the column. High pH could lead to an

injection spike caused by a rapid change in pH within the reaction flow cell. Unaltered MQ water from our system had a pH of ~6 and did not elute any manganese during the rinse cycle (Fig. 14), nor did it produce injection spikes that were too large. When the injection valve was switched to the elute position, the column was then eluted with the 0.0025 M HCl which quantitatively removed the manganese and delivered it to the detection cell in front of the PMT.

The sensitivity was dependent on the volume of sample that was passed through the column, and, therefore, on the column load time. The detector signal increased linearly with load times from 2 to 16 minutes for Mn standards in MQ-water (Fig. 15). However, the available sites on the 8-hydroxyquinoline column were quickly filled by the cations in seawater and this resulted in a much lower resin capacity in seawater than in MQ water. For the 1.0 cm 8-HQ column, the signal was linear only to a 4 minute load time and the available sites were saturated after about 8 minutes of seawater loading (Fig. 16). A 4 minute load time was used in the remaining work described here. The extraction efficiency of the 8-HQ columns was measured by placing two identical columns in line and loading the columns with seawater. After the 4 minute load was completed, the second column was then eluted with acid and the Mn determined. Any Mn not adsorbed by the first column would then be adsorbed by the second

column. The Mn extraction efficiency was approximately 80%
for seawater. The high reproducibility of the system
eliminated the need for efficiency yield tracers. Shorter
columns may be used in fresh water analysis since the
available sites on the column are unlikely to become saturated
(Fig. 15).

The column length also affected the flow characteristics
as well as the number of available binding sites. Longer
columns resulted in higher backpressure and lower flow rates
which reduced the sensitivity by broadening the elution peak.
Peak integration may be able to resolve the problem of longer
columns. Shorter columns may not have the binding site
capacity to reproducibly adsorb the manganese in the presence
of the other seawater cations (Fig. 17). A 1.5 cm column was
able to bind most of the manganese in a 4 minute load period,
but the 1.0 cm column had better elution characteristics.
Both column lengths were used during this study.

Interferences

Yamada et al. (9) reported no interference from 10^{-4} M
solutions of Co(II), Ni(II), Cu(II), Zn(II), Cr(III,VI),
Pb(II), Cd(II), Ag(I), Mo(VI), Al(III), Ca(II), F^-, Cl^-, Br^-,
I^-, CO_3^{2-}, PO_4^{3-}, SO_4^{2-}, NO_3^-, CH_3COO^-, $C_2O_4^{2-}$, and citric acid.
However, Fe(II), Fe (III) and Mg(II) did interfere, giving
signals that were 6% and 1% respectively of a 10^{-4} M Mn signal

but gave no interference at 10^{-5} M. Unfortunately, seawater contains 53.3 mM of Mg(II) and this would interfere significantly unless the Mg(II) was removed by rinsing the 8-HQ column with the MQ rinse. The interference effects of magnesium in seawater were very difficult to determine. The effect of 53 mM of Mg(II) AA standard was studied and resulted in a signal equivalent to approximately 1 nM Mn. Most of this signal disappeared after 45 seconds of MQ rinsing, but a small signal did remain. However this is signal is well within the certified value for manganese levels in the Mg(II) AA standard.

In addition to Mg, the following metals were analyzed to measure their effective interference: Co(II), Ni(II), Cu(II), Zn(II), Cr(VI), Pb(II), Cd(II), Ag(I), Mo(VI), Al(III), and Fe(II,III). Metal interferences were tested at levels that were five times greater than the maximum concentrations found in open ocean seawater (15). There were no significant interferences except for Mo(VI), Cu(II) and Fe(II) (Table 2). When Mo(VI) was analyzed at natural seawater levels, the interference was negligible.

Copper (II) gave a slight emission at a 6 nM level but at concentrations of 3 nM did not chemiluminesce. If high levels of Cu(II), (>5 nM), are likely to be encountered the copper can be complexed with tetraethylenepentamine, TEPA, and this complex will not adsorb onto the 8-HQ column. This ligand has a very high specificity for copper and also has an extremely

high binding constant for copper, approximately 17 orders of magnitude greater than the 8- hydroxyquinoline (46). The TEPA could be added directly to the sample or, to maintain sample integrity, it could be added to the MQ rinse where it strips the copper off the column but leaves the manganese behind (Table 3).

Iron (II) still interfered at 3 nM concentrations. Fortunately the kinetics of the oxidation of Fe(II) to Fe(III) are very fast and interfering amounts of Fe(II) should not accumulate under most seawater conditions. High Fe(II) concentrations, such as those found in hydrothermal fluids or anoxic systems might interfere with the manganese determinations. Iron interference could be reduced by the addition of Desferol, a siderophore, to the MQ wash (Carol Chin pers. comm.) in a manner similar to TEPA additions for Cu(II) interference. Desferol has a very high specificity for iron and could strip the iron off the 8-HQ column while leaving the manganese behind.

Standard additions, blanks, precision, and accuracy.

The system response to manganese was determined by making standard additions of Mn(II) to seawater samples. Deep seawater samples were chosen because they contain low levels of manganese. The resulting calibration curves were used to determine the concentrations of Mn in the other samples.

Deepwater samples were used for the standard additions in order to eliminate any potential problems from plankton or other large particulates that could clog the 8-HQ column and produce inconsistent results. Actual blank concentrations were determined using Mn free seawater because MQ water blanks do not take into account the matrix effects of seawater on the 8-HQ column and should not be used without careful evaluation. K. Bruland and L. Miller from U.C. Santa Cruz kindly provided us with a sample of trace metal clean seawater prepared by their laboratory. The trace metals were removed from the seawater by irradiating the seawater with ultraviolet light (to oxidize metal binding ligands) and then passing it through a series of ion-exchange columns to remove manganese (47). The blank determined with this Mn free seawater ranged from 0.15-0.2 nM manganese for a 4 minute sample load. This value was almost at the detection limit for the 4 minute load and indicates that the technique and sample handling procedures are not very susceptible to contamination. Due to the limited supply of trace metal clean seawater, the system blank was only determined for a 4 minute load time. MQ blanks were run on every series of analyses and were used to detect contamination and analysis problems. The signal from the Milli-Q blank was equivalent to 0.3 nM. The detection limit was determined as three times the standard deviation of the trace metal free blank. For this technique, the detection

limit depended upon the load time and for a 4 minute load, the detection limit was 0.1 nM.

Samples that were acidified for storage required the addition of high purity NH₄OH to bring the pH back up to pH 8. The addition of the acid and the base caused a significant blank, 0.2 nM. The elution characteristics of the pH adjusted samples were also different than fresh seawater samples. Therefore, samples should be analyzed as soon as possible after collection to avoid problems with sample storage and pH adjustment.

Standard additions for seawater analyses were usually made using 0, 0.5, 1.0, 2.0, and 4.0 nM additions (Fig. 5). For this system, the detector response to manganese standard additions was very reproducible, with a slope of approximately 325 counts sec^{-1} nM^{-1} and a relative standard deviation of approximately 5% (Fig. 18). This slope depends on many parameters such as the flow cell, PMT efficiency, and flow rates and will vary from system to system. System response did vary somewhat from day to day, but during a given analysis period the response was very stable. The correlation coefficient for the curves were almost always greater than 0.99. The detector response was linear over three orders of magnitude from 0.1 nM to a concentration of over 100 nM Mn. The precision of replicate analyses was also very good with a sample standard deviation of ±3% (n=3) for both seawater

standards and samples (Fig. 5).

The accuracy of the FIA-CL system was determined using Coastal Atlantic Surface Seawater (CASS-1) and North Atlantic Surface Seawater (NASS-1) standard seawater. These standards have been rigorously analyzed by a number of analytical techniques for many of the trace metals including manganese. The acidified CASS-1 and NASS-1 standards were adjusted to pH 8 with NH_4OH prior to analysis. The results are presented in Table 1.

The excellent agreement with the CASS-1 trace metal standard verifies the accuracy of the FIA-CL technique at the higher Mn concentrations. The agreement with the low Mn NASS-1 standard was not very good. However, this standard is very old and has not been stored under rigorously "clean" conditions and most likely contaminated. New NASS standard will be analyzed as soon as possible.

Comparison with Oceanographically Consistent Mn Analyses.

Boyle et al. (3) have stated that analyses of trace metals in seawater should not be accepted unless they meet two criteria, "The primary criteria must be interlaboratory agreement and the oceanographic consistency of the data themselves: detailed profiles should show smooth variations related to hydrographic and chemical features displayed by conventionally measured properties." In order to determine if

the FIA-CL method described here met these criteria, Mn samples were collected and analyzed at sea off the California coastline during June 1989. The hydrographic and manganese data for the stations are presented below in Tables 4-9. Station 1 was closest to shore while Station 7 was furthest offshore.

Station 4 and Station 5 were located approximately 70 km away from nearby stations where both Landing and Bruland (2) and Martin et al. (1) determined manganese concentrations. Both of these sets of analyses were performed in a shore based lab by GFAAS after concentrating the samples with Chelex-100 resin. Figure 19 shows a vertical profile of Mn concentrations at Station 4 analyzed at sea with the FIA-CL method and a Mn profile reported by Martin et al. (1). Figure 20 exhibits the Mn profile of Station 5 analyzed at sea and a profile from Landing and Bruland (2) from a nearby station. All sets of data show the classic manganese profile of surface maxima, subsurface minima, midwater maxima associated with the oxygen minimum, and decreasing deeper values. The Martin data and our FIA-CL Station 4 also exhibit another subsurface maxima just below the photic zone at approximately 100 m. This maxima does not seem to be a constant feature and could easily be a transient effect of local hydrographic and biological conditions. The excellent agreement of the FIA-CL manganese values with the reliable data of Martin et al. and

Landing and Bruland confirm the reliability of the this analytical technique.

CONCLUSIONS

The biogeochemical cycling of manganese is very complex, due to the myriad of processes affecting its distribution. These processes include atmospheric, fluvial, and hydrothermal input; incorporation into phytoplankton; photochemical oxidation; scavenging and regeneration; microbially mediated redox transformations; advection and diffusion from sediments; and sedimentation. Manganese is a powerful tracer of these processes and many more analyses and studies must be conducted in order to elucidate the parameters that control the manganese distribution in seawater. This necessitates the development of fast, sensitive, inexpensive, and portable analytical techniques.

This paper presents a new technique for the analysis of manganese in seawater at natural concentrations. Flow injection analysis coupled with chemiluminescence detection is utilized to permit rapid, inexpensive, portable, and precise determinations of manganese with very little sample handling or processing. This technique has been adapted to shipboard analysis and has produced vertical profiles which are in excellent agreement with previous results.

LITERATURE CITED

1. J.H. Martin, G.A. Knauer, and W.W. Broenkow, Deep-Sea Res., 32 (1985) 1405.

2. W.M. Landing and K.W. Bruland, Geochim. Cosmochim. Acta, 51 (1987) 29.

3. E.A. Boyle and J.M. Edmond, Anal. Chim. Acta, 91 (1977) 189.

4. K.W. Bruland, R.P. Franks, G.A. Knauer, and J.H. Martin, Anal. Chim. Acta, 105 (1979) 233.

5. W.M. Landing and K.W. Bruland, Earth Planet. Sci. Lett., 49 (1980) 45.

6. L. Mart, H.W. Nürnberg, and D. Dyrssen, in C.S. Wong et al. (Eds.), Trace Metals in Seawater, Plenum Press, New York, 1983.

7. C.I. Measures and J.M. Edmond, Nature (London), (1982) 361.

8. G.P. Klinkhammer, and M.L. Bender, Earth Planet. Sci. Lett., 46 (1980) 361.

9. M. Yamada, S. Kamiyama, and S. Suzuki, Chemistry Lett., (1985) 1597.

10. K.S. Johnson and R.L. Petty, Anal. Chem., 54 (1982) 1185.

11. J. Thomsen, K.S. Johnson, and R.L. Petty, Anal. Chem., 55 (1983) 2378.

LITERATURE CITED (cont.)

12. K.S. Johnson and R.L. Petty, Limnol. Oceanogr., 28 (1983) 1260.

13. K.S. Johnson, C.M. Sakamoto-Arnold, S.W. Wilson, and C.L. Beehler, Anal. Chim. Acta, 201, (1987) 83.

14. P.J. Statham and R. Chester, Geochim. Cosmochim. Acta, 52 (1988) 2433.

15. K.W. Bruland, in J.P. Riley, R. Chester, (Eds.),Chemical Oceanography, vol. 8, chapter 45, Academic, London, 1983.

16. W.G. Sunda and S.A. Huntsman, Deep-Sea Res., 35 (1988) 1297.

17. W.G. Sunda, S.A. Huntsman, and G.R. Harvey, Nature, 301 (1983) 234.

18. C.R. Myers and K.H. Nealson, Sci., 240 (1988) 1319.

19. S. Emerson, S. Kalhorn, L. Jacobs, B.M. Tebo, K.H. Nealson, and R.A. Rosson, Geochim. Cosmochim. Acta, 46 (1982) 1073.

20. J.P. Cowen and M.W. Silver, Sci., 224 (1984) 1340.

21. J.P. Cowen and K.W. Bruland, Deep-Sea Res., 32 (1985) 253.

22. J.H. Martin and G.A. Knauer, Earth and Planet. Sci. Lett., 67 (1984) 35.

23. J.H. Martin and G.A. Knauer, J. Mar. Res., 40 (1982) 1213.

LITERATURE CITED (cont.)

24. G.P. Klinkhammer and A. Hudson, Earth and Planet. Sci. Lett., 79 (1986) 241.

25. R.F. Weiss, Earth and Planet. Sci. Lett., 37 (1977) 257.

26. M.L. Bender, G.P. Klinkhammer, and D.W. Spencer, Deep-Sea Res., 24 (1977) 799.

27. E.V. Grill, Geochim. Cosmochim. Acta, 46 (1982) 2435.

28. K.W. Bruland and R.P. Franks, in C.S. Wong et al. (Eds.), Trace Metals in Seawater, Plenum Press, New York, (1983), 395.

29. R. Chester and M.J. Hughes, Chem. Geol., 2 (1967) 249.

30. D.W. Eggiman and P.R. Betzer, Anal. Chem., 48 (1976) 822.

31. F.M.M. Morel and R.J.M. Hudson, in W. Stumm, (Ed.), Chemical Processes in Lakes, Wiley, New York, 1985, p251.

32. K.H. Coale, TOS Meeting Abstract, 1989.

33. J.H. Martin, G.A. Knauer, D.M. Karl, and W.W. Broenkow, Deep-Sea Res.,34 (1987) 267.

34. K.S. Johnson, in press

35. D. Diem and W. Stumm, Geochim. Cosmochim. Acta., 48 (1984) 1571.

36. J.P. Cowen, G.J. Massoth, and E.T. Baker, Nature, 322 (1986) 169.

LITERATURE CITED (cont.)

37. J. Ruzicka and E. H. Hansen, in J.D. Winefordner ed., Flow Injection Analysis, 2nd ed., vol 62 Chemical Analysis, John Wiley & Sons New York, 1988.

38. M. Yamada, A. Sudo, and S. Suzuki, Chemistry Lett., (1985) 801.

39. C.M. Sakamoto-Arnold and K.S. Johnson, Anal. Chem., 59 (1987) 1789.

40. P.M. Stout, K.H. Coale, K.S. Johnson, C.M. Sakamoto-Arnold (in press).

41. A.O. Jacintho, E.A.G. Zagatto, F. Bergamin, F.J. Krug, B.F. Reis, R.E. Burns, and B.R. Kowalski, Anal. Chim. Acta, 130 (1981) 243.

42. J. Wang, H.D. Dewald, and B. Greene, Anal. Chim. Acta, 146 (1983) 45.

43. O.S. Fedorova, S.E. Olkin, and V.M. Berdnikov, Z. phys. Chemie, Leipzig 263 (1982) 3, 529.

44. W.L. Hinze, in K.L. Mittal (Ed.), Solution Chemistry of Surfactants, vol. 1, Plenum, New York and London, 1979, p 79.

45. W.M. Landing, C. Haraldson, and N. Paxeus, Anal. Chem., 53 (1986) 3031.

46. A.E. Martell and R.M. Smith, Critical Stability Constants, Plenum: New York, 1974.

47. K.H. Coale and K.W. Bruland, Limnol. Oceanogr., 33 (1988) 1084.

TABLE 1

FIA-CL analysis of CASS-1 and NASS-1 Standard Seawater.

	CASS	NASS
STANDARD VALUE	41.3 ± 3.1 nM	0.40 ± .13 nM
FIA-CL VALUE	42.9 ± 2.8 nM (n=4)	0.92 ± .12 nM (n=3)

Reported errors represent one standard deviation ($\sigma=1$).

TABLE 2

Effect of trace metal interference relative to a 5 nM manganese signal. 100% signal is equivalent to 5 nM Mn,

Interferant	% signal relative to 5 nM Mn
25 nM Cr(II)*	1
500 nM Mo(VI)*	15
100 nM Mo(VI)	1
1 nM Pb(II)*	0
45 nM Zn(II)*	3
5 nM Zn(II)	0
500 pM Ag(II)*	0
5 nM Cd(II)*	0
200 nM Al(III)*	0
1 nM Co(II)*	1
60 nM Ni(II)*	1
15 nM Fe(II)*	50
3 nM Fe(II)	5
15 nM Fe(III)*	1
30 nM Cu(II)*	30
6 nM Cu(II)	5
3 nM Cu(II)	2

* denotes concentrations five times greater than maximum oceanic values (11)

TABLE 3

Effect of tetraethylenepentamine (TEPA) addition to sample and to MQ column wash. 100% signal is equivalent to 5 nM Mn. TEPA concentration = 0.4μM.

Species	SAMPLE TEPA ADDED (μl/l OF SAMPLE)	MQ WASH TEPA ADDED (μl/l MQ)	RELATIVE SIGNAL (%)
5 nM Mn(II)	0		100
5 nM Mn(II)	100		99
30 nM Cu(II)	0		40
30 nM Cu(II)	100		1
5 nM Mn(II) + 30 nM Cu(II)	0		120
5 nM Mn(II) + 30 nM Cu(II)	100		106
5 nM Mn(II) + 30 nM Cu(II)	200		101
5 nM Mn(II)		0	100
5 nM Mn(II)		100	100
5 nM Mn(II)		200	98
5 nM Mn(II) + 30 nM Cu(II)		0	120
5 nM Mn(II) + 30 nM Cu(II)		100	112
5 nM Mn(II) + 30 nM Cu(II)		200	102
5 nM Mn(II) + 30 nM Cu(II)		300	96

TABLE 4.

Hydrographic and manganese data for PS89 Station 1 (36° 25'N, 121° 57'W). Samples collected and analyzed at sea by FIA-CL on June 1, 1989.

DEPTH (m)	POT TEMP (°C)	SALINITY (‰)	Sigma-t	OXYGEN (µM)	Mn (nM)
1	10.45	33.92	26.03	251	3.47
5	9.82	33.93	26.15	243	3.47
10	9.04	33.94	26.28	143	2.51
15	8.66	33.98	26.43	111	2.04
20	8.46	34.01	26.45	106	1.60
30	8.40	34.02	26.47	99	2.04
40	8.37	30.03	26.47	102	1.79
50	8.33	34.04	26.47	65	1.74
60	8.34	34.04	26.47	97	1.62
70	8.34	34.04	26.47	121	1.51
80	8.34	34.04	26.47	133	1.36
90	8.35	34.04	26.47	126	1.61

Bottom depth = 95 m.

TABLE 5.

Hydrographic and manganese data for PS89 Station 2 (36° 25'N, 122° 00'W). Samples collected and analyzed at sea by FIA-CL on June 2, 1989.

DEPTH (m)	POT TEMP (°C)	SALINITY (‰)	Sigma-t	OXYGEN (µM)	Mn (nM)
1	11.75	33.82	25.72	332	5.90
5	11.42	33.82	25.78	324	5.05
10	10.78	33.88	25.94	266	4.02
20	10.03	33.89	26.08	206	3.16
30	9.35	33.93	26.22	173	3.11
50	8.79	33.95	26.33	116	2.55
75	8.56	33.97	26.38	108	1.91
100	8.47	34.01	26.42	105	2.00
200	8.06	34.10	26.56	78	1.88
300	7.77	34.13	26.63	88	2.07
350	7.20	34.19	26.75	52	2.50
400	6.89	34.21	26.81	44	2.64

Bottom depth = 420 m.

TABLE 6.

Hydrographic and manganese data for PS89 Station 3 (36° 26'N, 122° 08'W). Samples collected and analyzed at sea by FIA-CL in June 2, 1989.

DEPTH (m)	POT TEMP (°C)	SALINITY (‰)	Sigma-t	OXYGEN (µM)	Mn (nM)
1	11.39	33.73	25.72	345	–
5	11.34	33.75	25.74	343	–
10	10.29	33.75	25.93	276	–
20	9.94	33.80	26.03	232	5.07
30	9.61	33.81	26.09	190	4.18
50	8.94	33.88	26.25	126	1.13
75	8.51	33.98	26.40	122	0.94
100	8.45	34.00	26.42	118	0.84
300	7.56	34.16	26.68	56	1.49
500	6.22	34.24	26.93	41	1.46
600	5.37	34.30	27.08	19	1.63
750	4.67	34.38	27.22	23	1.67

Bottom Depth = 760 m.

TABLE 7.

Hydrographic and manganese data for PS89 Station 4 (36° 25'N, 122° 30'W). Samples collected and acidified at sea on June 4, 1989. Samples analyzed in lab by FIA-CL on July 17, 1989.

DEPTH (m)	POT TEMP (°C)	SALINITY (‰)	Sigma-t	OXYGEN (µM)	Mn (nM)
1	14.20	33.32	24.85	257	—
5	14.19	33.32	24.85	258	—
10	14.10	33.36	24.90	260	1.62
20	13.11	33.45	25.17	272	1.77
30	12.19	33.54	25.42	268	2.91
40	11.02	33.61	25.69	257	3.36
50	9.72	33.58	25.89	177	1.31
60	9.45	33.69	26.02	157	1.44
80	9.29	33.75	26.09	145	1.33
100	9.05	33.87	26.23	125	1.49
150	8.35	34.03	26.46	107	2.39
200	7.97	34.10	26.57	82	1.31
300	7.31	34.17	26.72	50	0.99
400	6.67	34.23	26.86	32	1.29
500	6.01	34.26	26.96	23	1.47
600	5.42	34.30	27.07	16	1.16
700	4.92	34.36	27.17	13	1.26
800	4.45	34.40	27.26	19	0.76
900	4.28	34.41	27.29	26	(3.71)[a]
1000	4.05	34.43	27.33	18	1.32
1200	3.49	34.48	27.42	26	0.69
1500	2.76	34.53	27.53	47	0.79
1750	2.30	34.57	27.60	62	0.59
2000	1.91	34.60	27.66	63	0.93

Bottom depth = 2700 m.

[a]VALUE DELETED FROM VERTICAL PROFILE

TABLE 8.

Hydrographic and manganese data for PS89 Station 5 (36° 25'N, 123° 08'W). Samples collected and analyzed at sea by FIA-CL on June 4, 1989.

DEPTH (m)	POT TEMP (°C)	SALINITY (‰)	Sigma-t	OXYGEN (µM)	Mn (nM)
1	14.13	33.28	24.83	274	3.17
5	14.14	33.28	24.83	275	3.15
10	14.12	33.28	24.83	275	3.07
20	13.57	33.32	24.98	275	3.25
30	12.43	33.34	25.22	266	2.66
40	11.32	33.37	25.45	245	2.34
50	10.74	33.39	25.57	229	1.92
60	9.90	33.54	25.83	193	1.14
80	9.40	33.67	26.01	156	0.87
100	9.04	33.74	26.13	125	0.77
150	8.24	33.97	26.43	123	0.64
200	7.79	34.06	26.56	95	0.71
300	6.71	34.08	26.74	57	0.76
400	6.34	34.20	26.87	32	1.21
500	5.76	34.25	26.99	18	1.18
600	5.03	34.28	27.10	11	1.06
700	4.77	34.35	27.19	13	1.21
800	4.45	34.38	27.25	16	1.04
900	4.09	34.42	27.32	19	1.09
1000	3.80	34.45	27.37	23	0.95
1200	3.28	34.49	27.45	36	0.75
1500	2.65	34.54	27.55	51	0.91
1750	2.26	34.57	27.61	63	0.61
2000	1.92	34.60	27.66	82	0.64

Bottom depth = 3200 m.

TABLE 9.

Hydrographic and manganese data for PS89 Station 7 (36° 25'N, 124° 20'W). Samples collected and analyzed at sea by FIA-CL on June 5, 1989.

DEPTH (m)	POT TEMP (°C)	SALINITY (‰)	Sigma-t	OXYGEN (µM)	Mn (nM)
300	7.21	34.05	26.64	89	0.67
400	6.40	34.13	26.82	56	0.91
500	5.78	34.20	26.95	26	1.08
600	5.16	34.24	27.05	19	1.21
700	4.80	34.31	27.15	14	1.38
800	4.45	34.36	27.23	18	1.06
900	4.05	34.40	27.31	43	1.07
1000	3.73	34.43	27.36	22	0.87
1200	3.30	34.48	27.44	41	0.79
1500	2.66	34.53	27.54	51	0.75
1750	2.24	34.57	27.61	65	0.89
2000	1.95	34.59	27.65	80	0.86

Bottom depth = 3900 m.

MANGANESE CYCLE IN SEAWATER
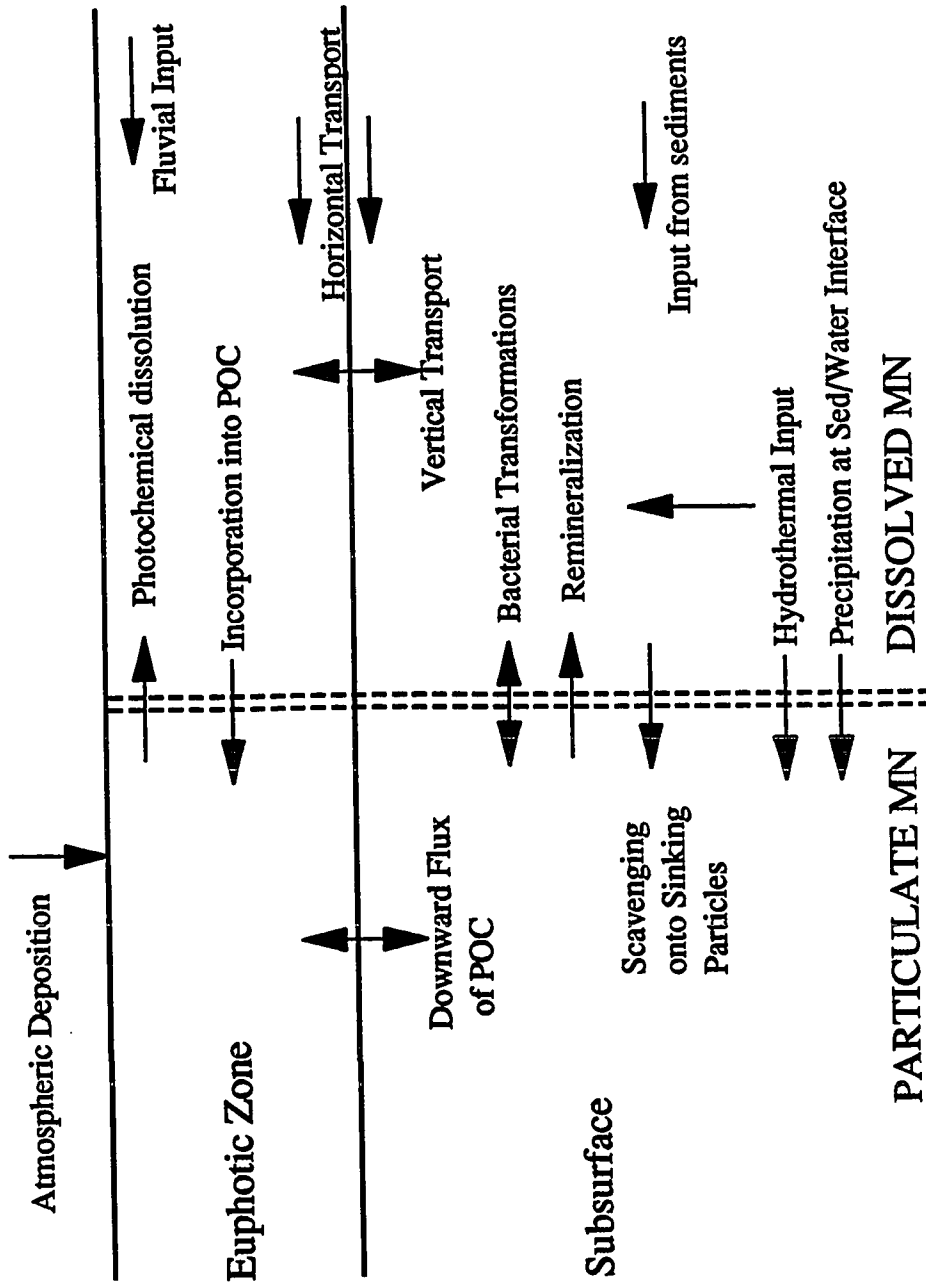
Figure 1. Manganese biogeochemical cycle.
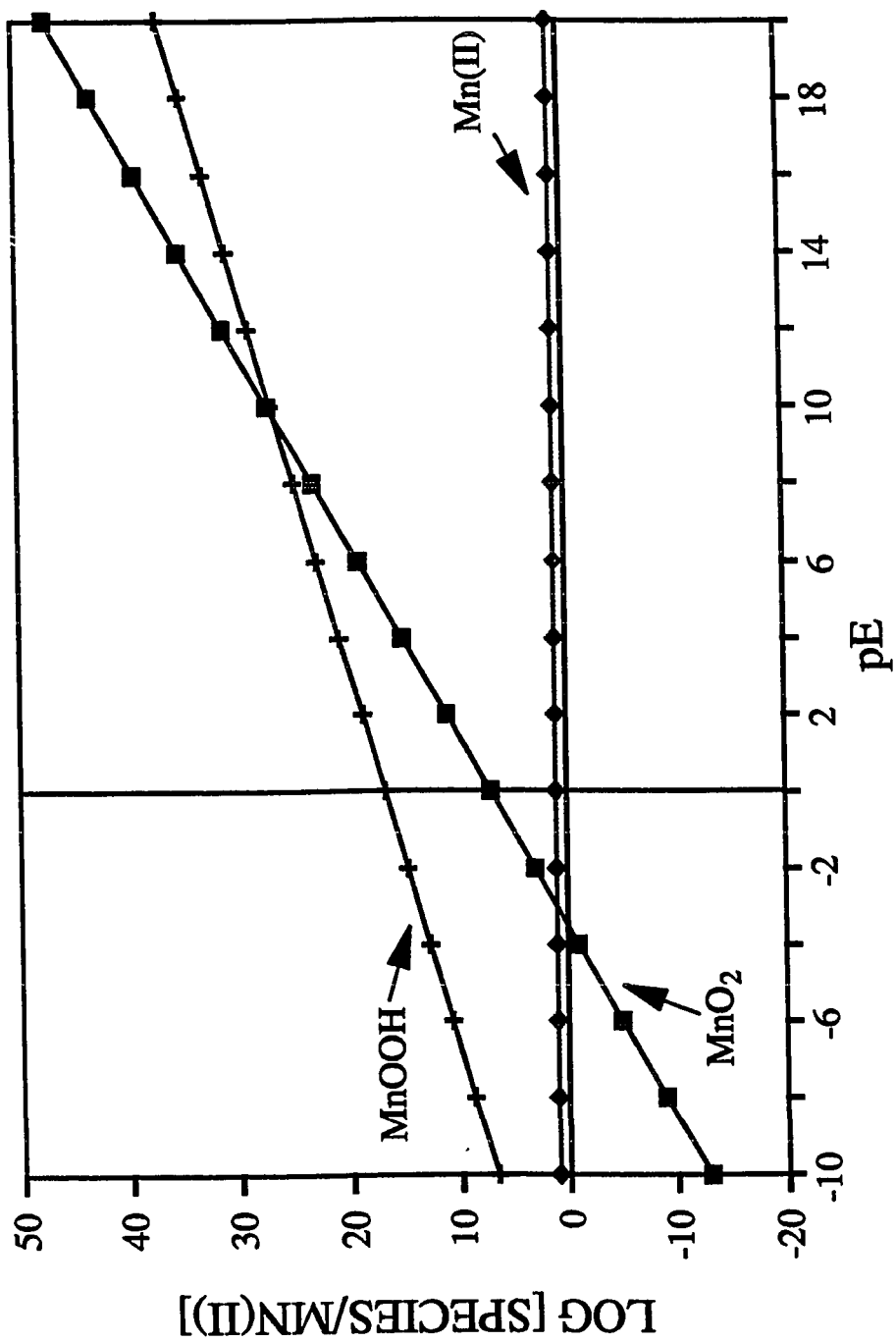
Figure 2. pE diagram for 1 nM Mn(II) at pH 8.0
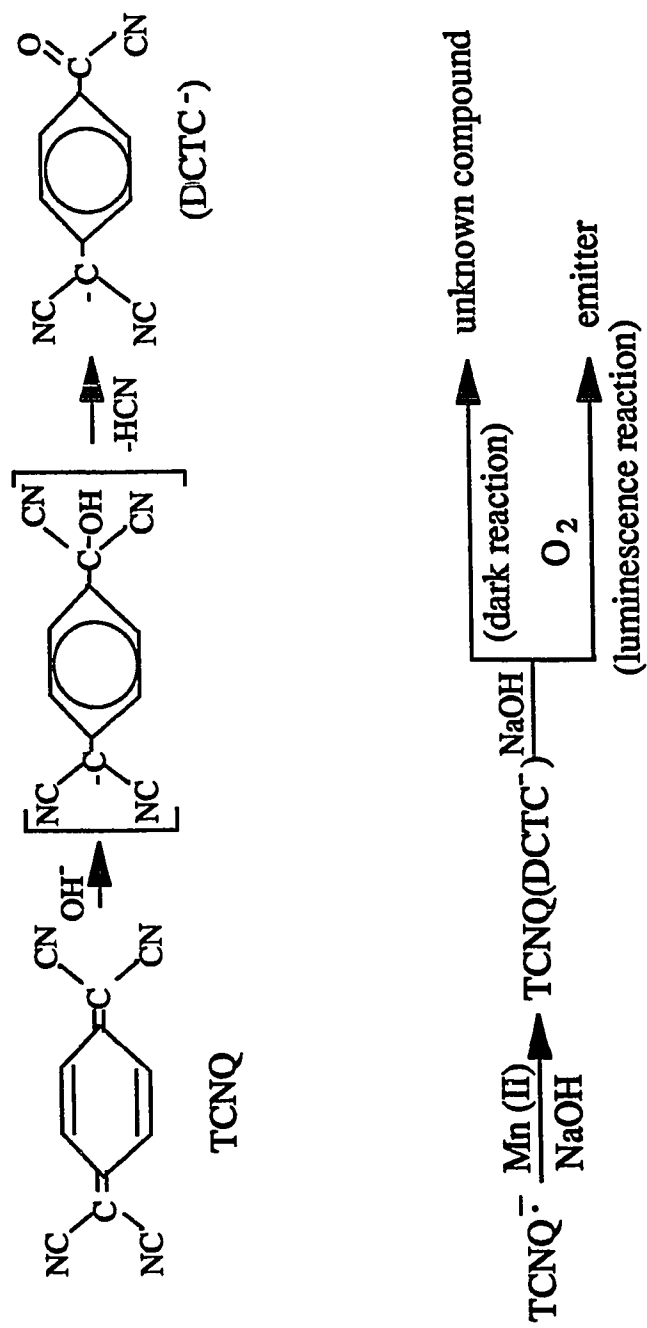
Figure 3. Reaction scheme for the Mn catalyzed oxidation of TCNQ.
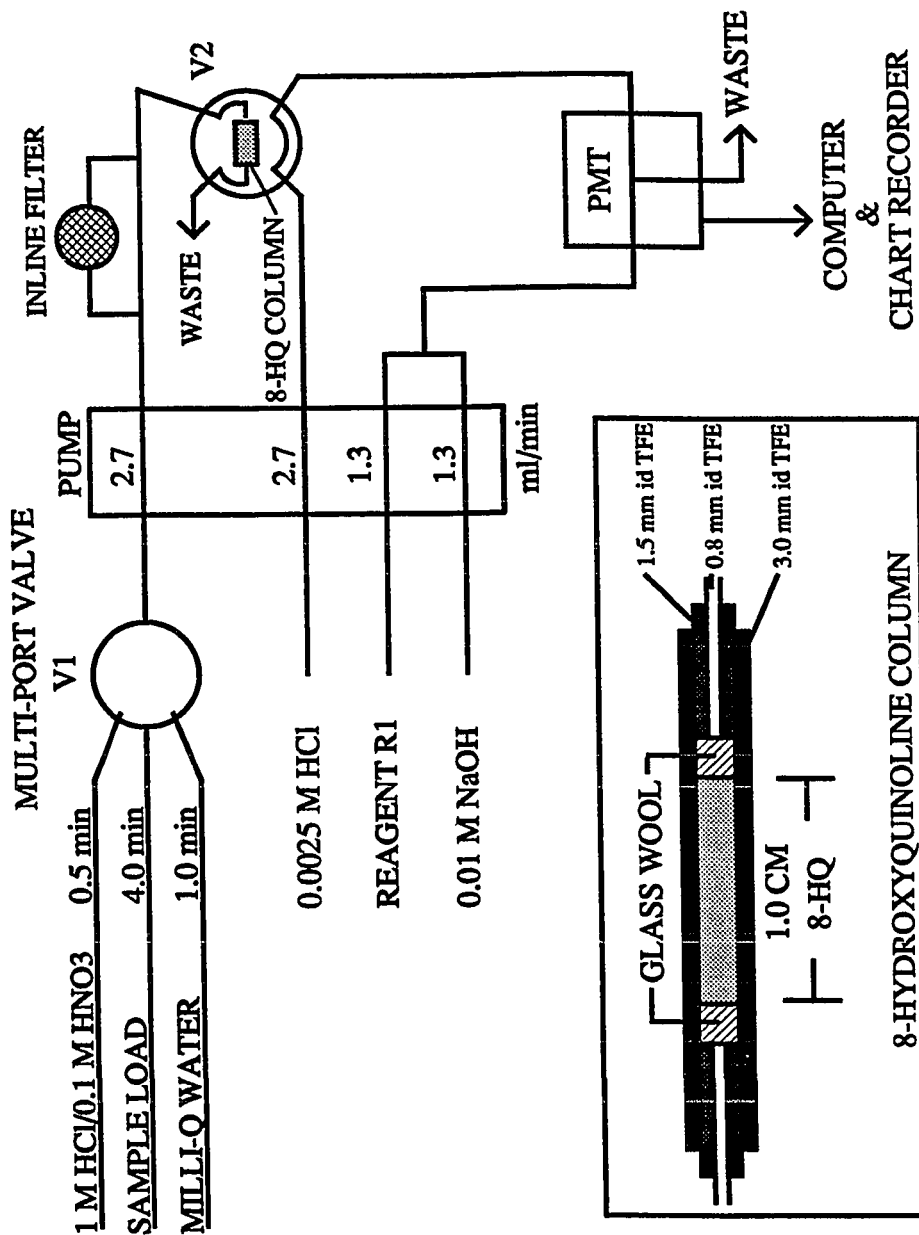
Figure 4. Schematic diagram of FIA-CL manifold.
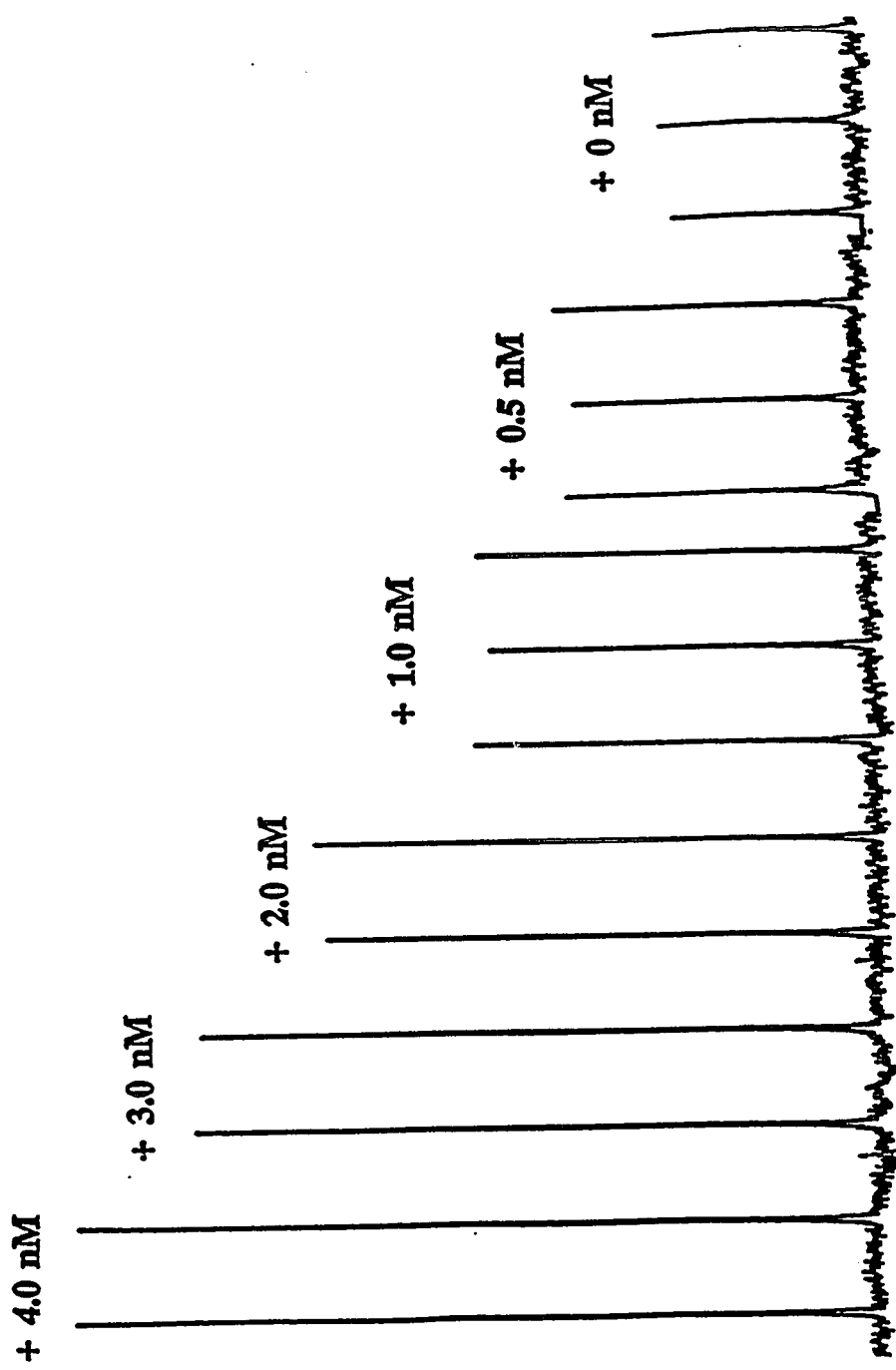
Figure 5. Recorder output of standard additions of Mn to a 1.09 nM seawater sample.
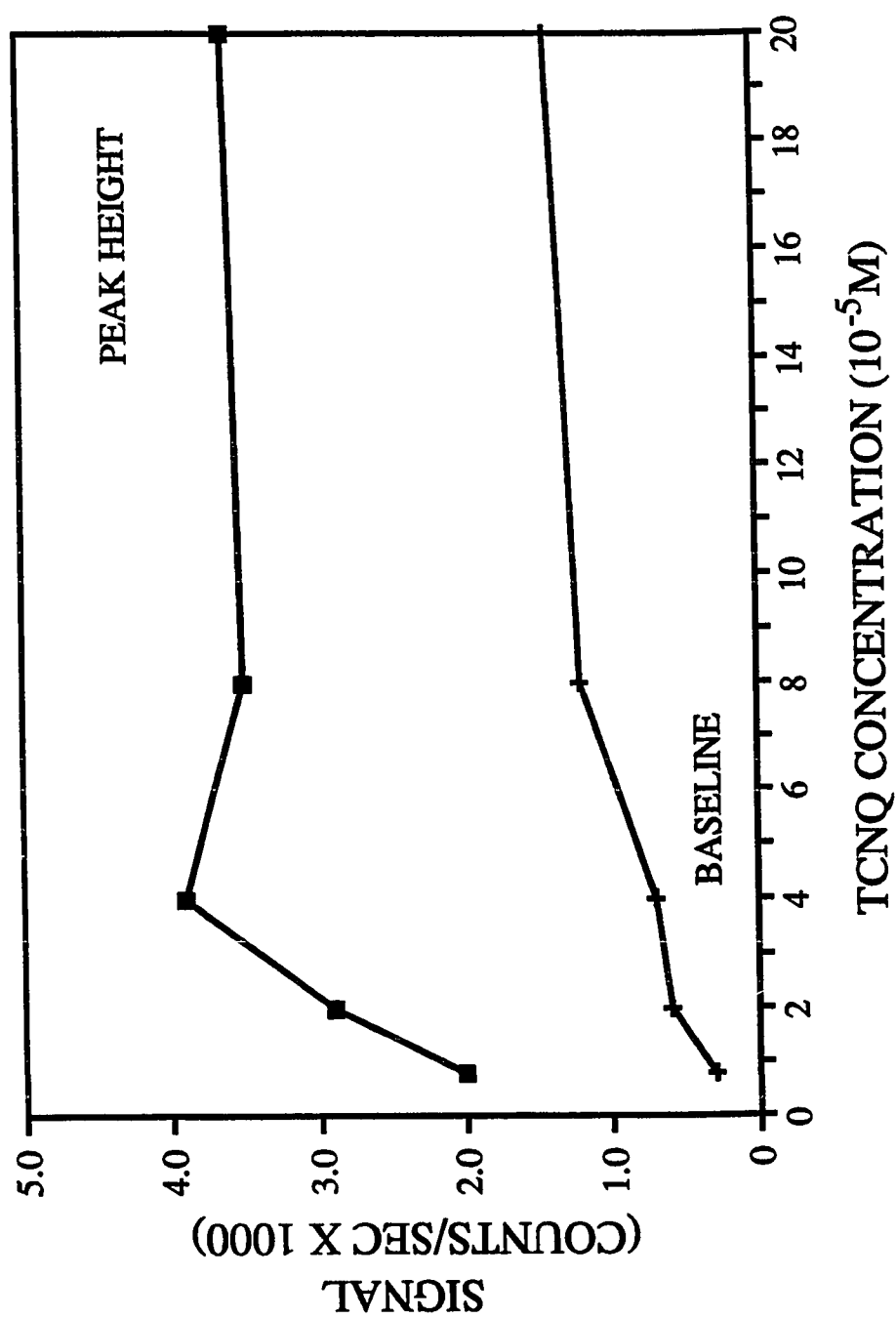
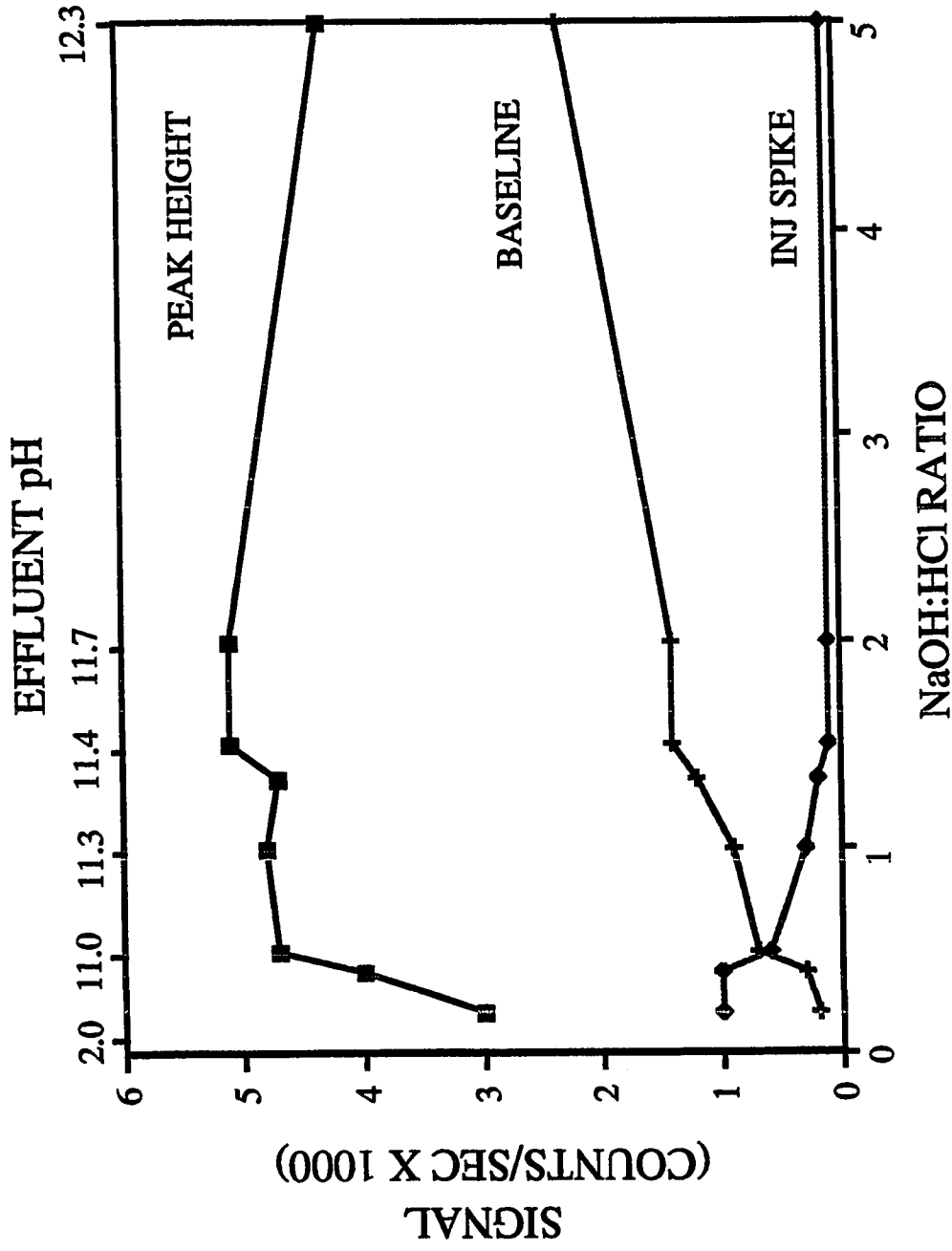Figure 6. Effect of TCNQ concentration on the signal and baseline of a 50 nM Mn seawater sample. 5×10^{-5} M TCNQ was chosen for analysis.
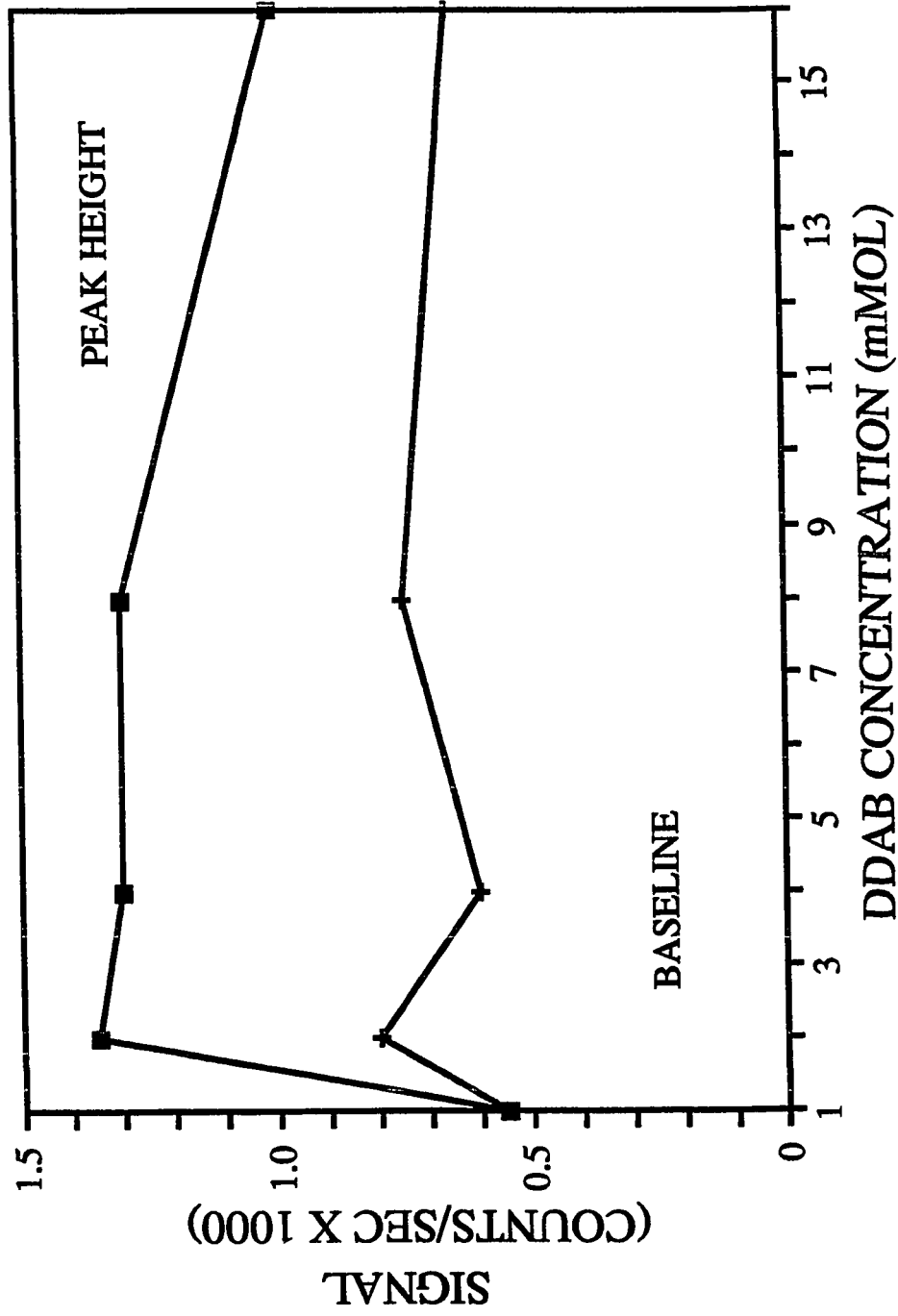
Figure 7. Effect of DDAB concentration on the signal and baseline of a 10 nM Mn seawater sample.
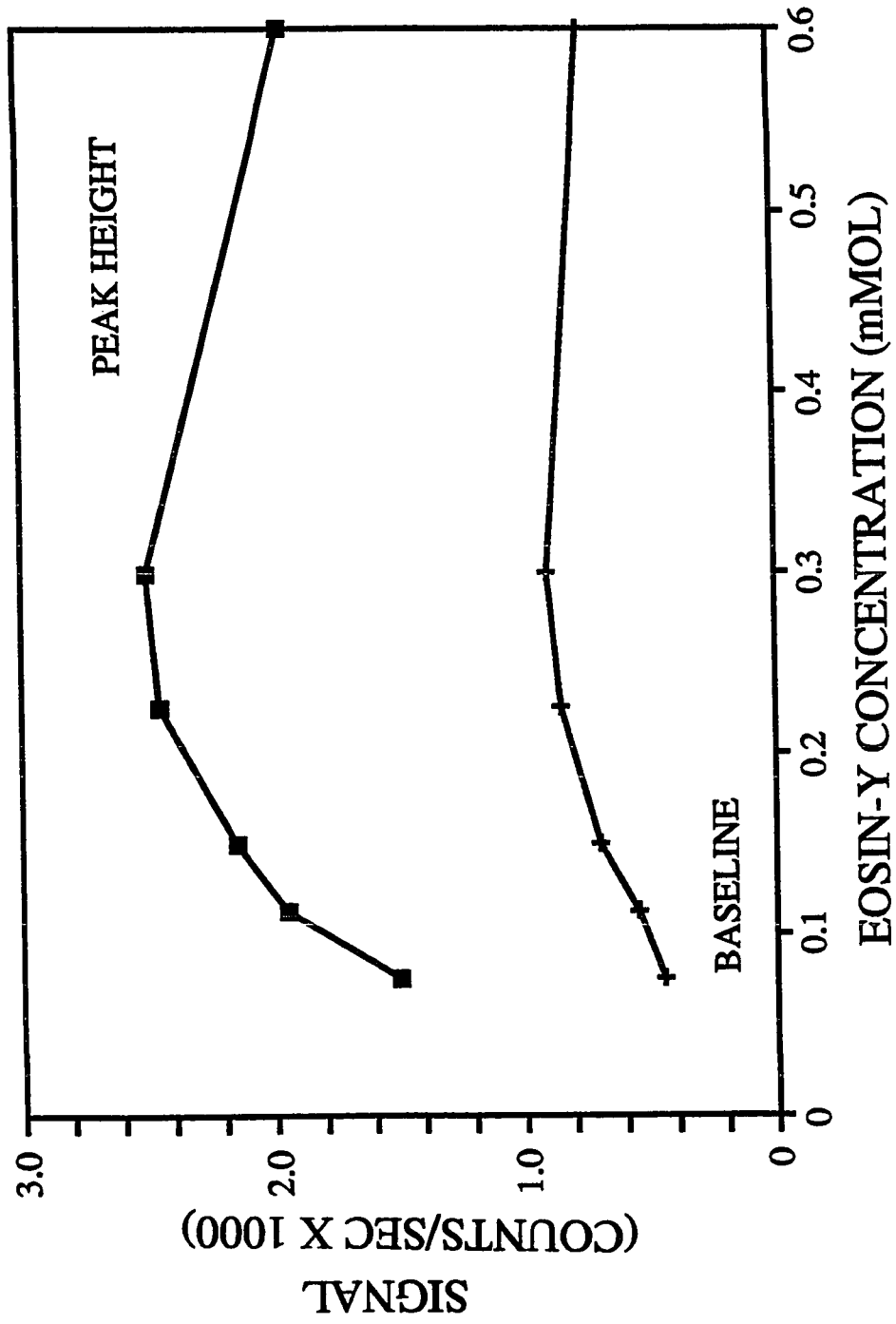
Figure 8. Effect of Eosin-Y concentration on the signal and baseline of a 5 nM Mn seawater sample.

Figure 9. Effect of NaOH:HCl ratio and effluent pH on the signal, baseline, and injection spike of a 50 nM Mn seawater sample.
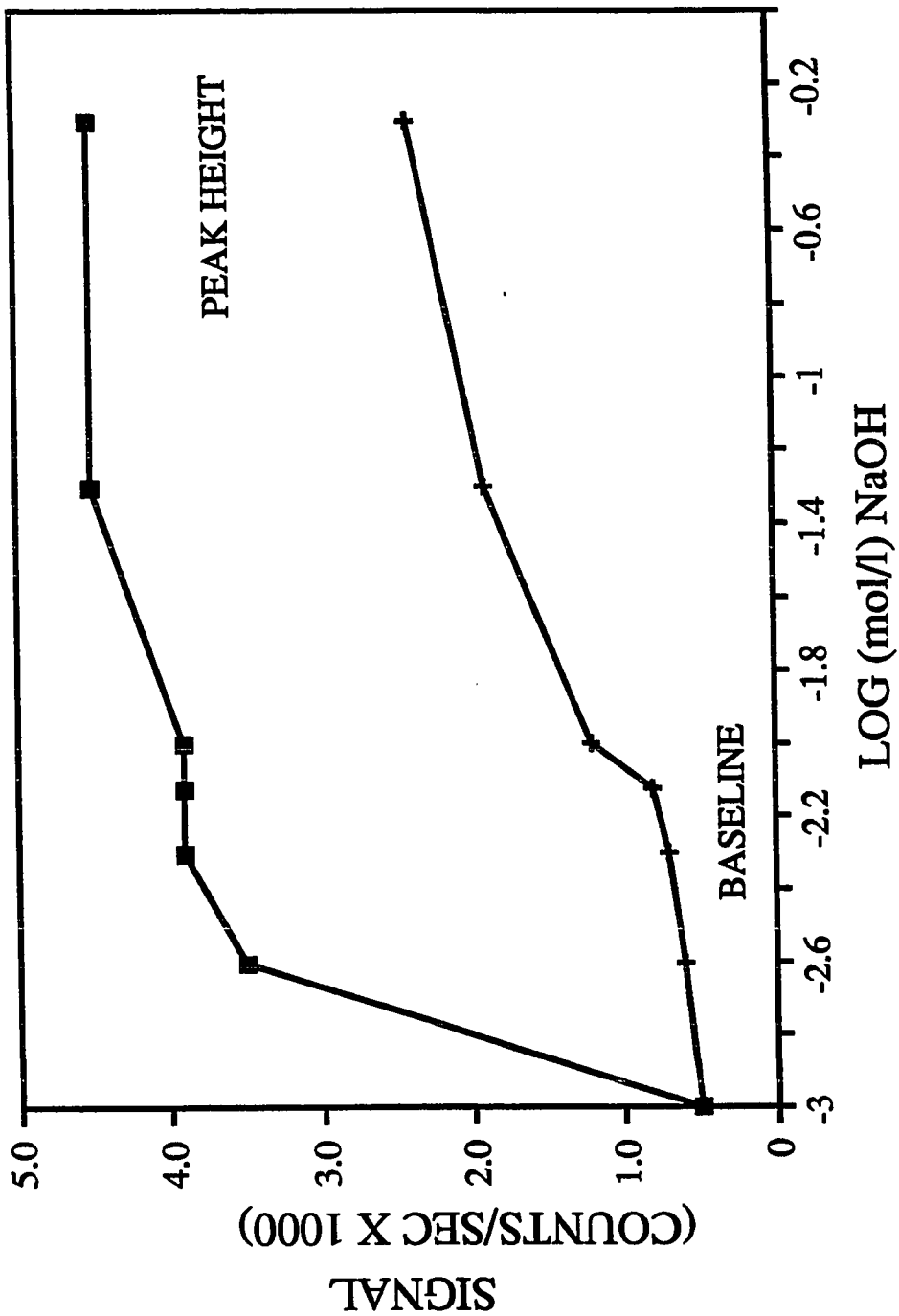
Figure 10. Effect of NaOH concentration on the signal and baseline of a 50 nM Mn seaater sample. 0.005 M NaOH was originally chosen for analysis. To reduce reagent consumption, 0.01 M NaOH at half the original flow rate was used for later analysis.
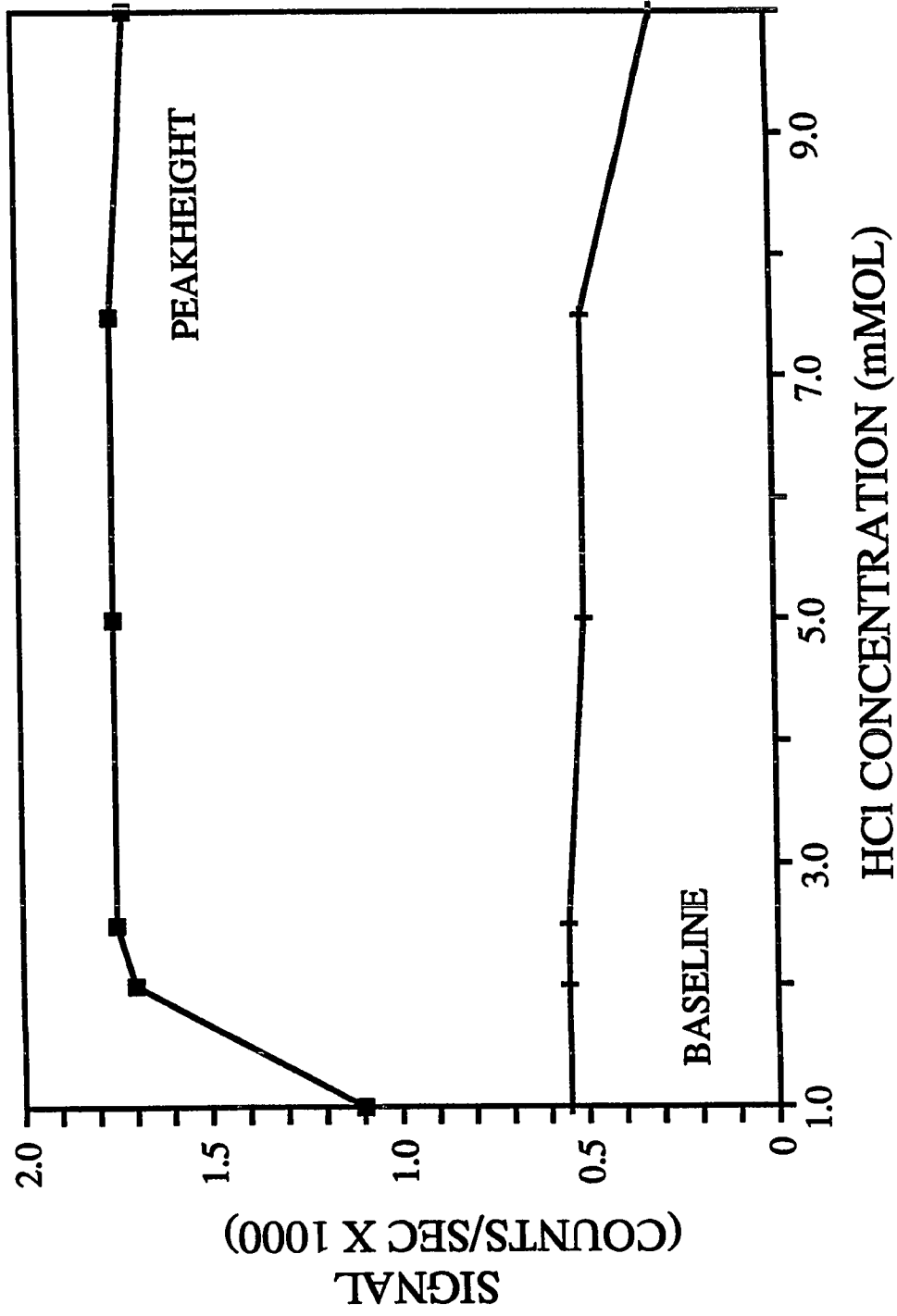
Figure 11. Effect of HCl concentration on the signal and baseline of a 5 nM Mn seawater sample. 0.0025 M HCl was chosen for analysis.
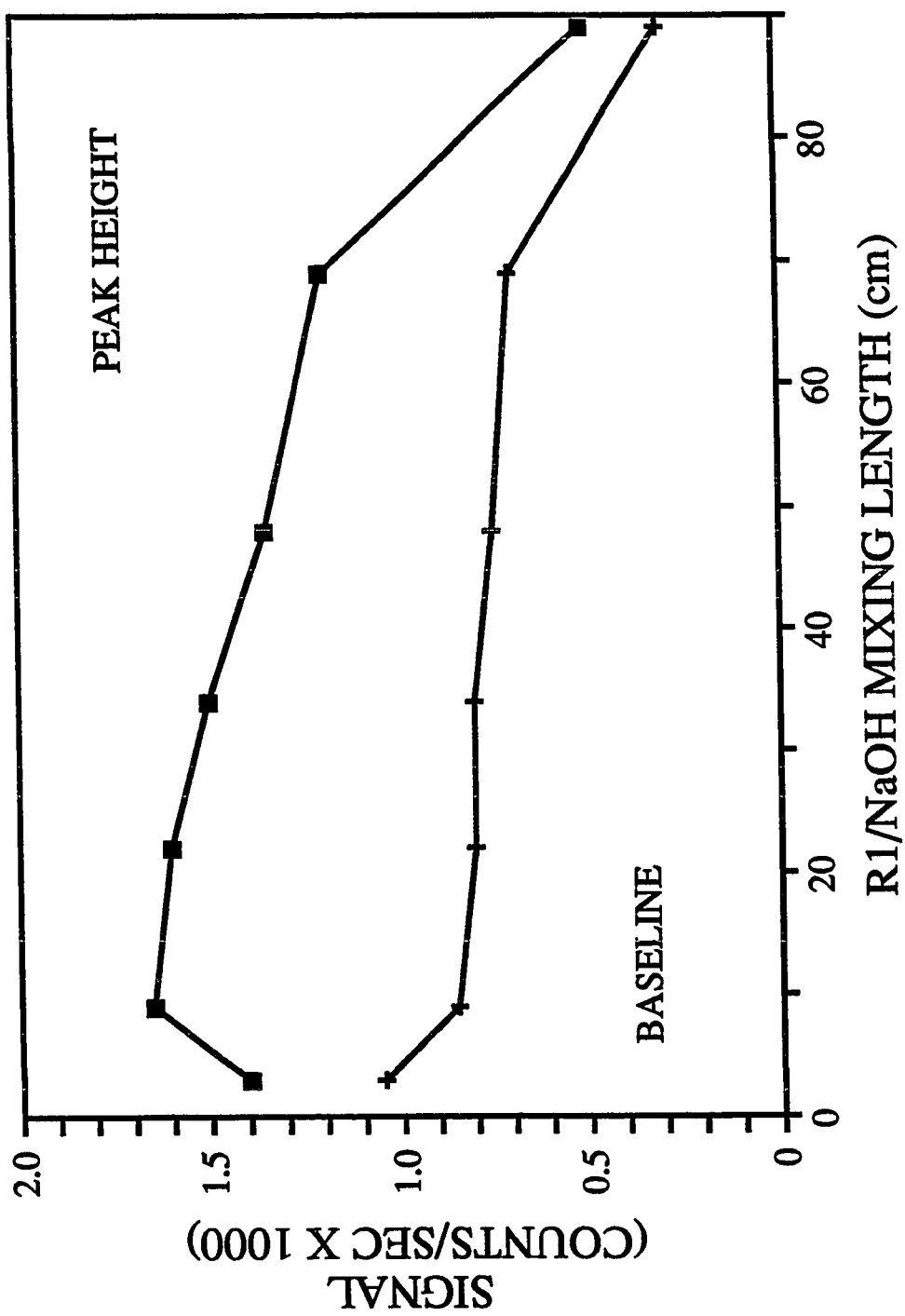
Figure 12. Effect of R1/NaOH mixing length on the signal and baseline of a 2 nM Mn seawater sample. A mixing length of 9 cm. was used during analysis.
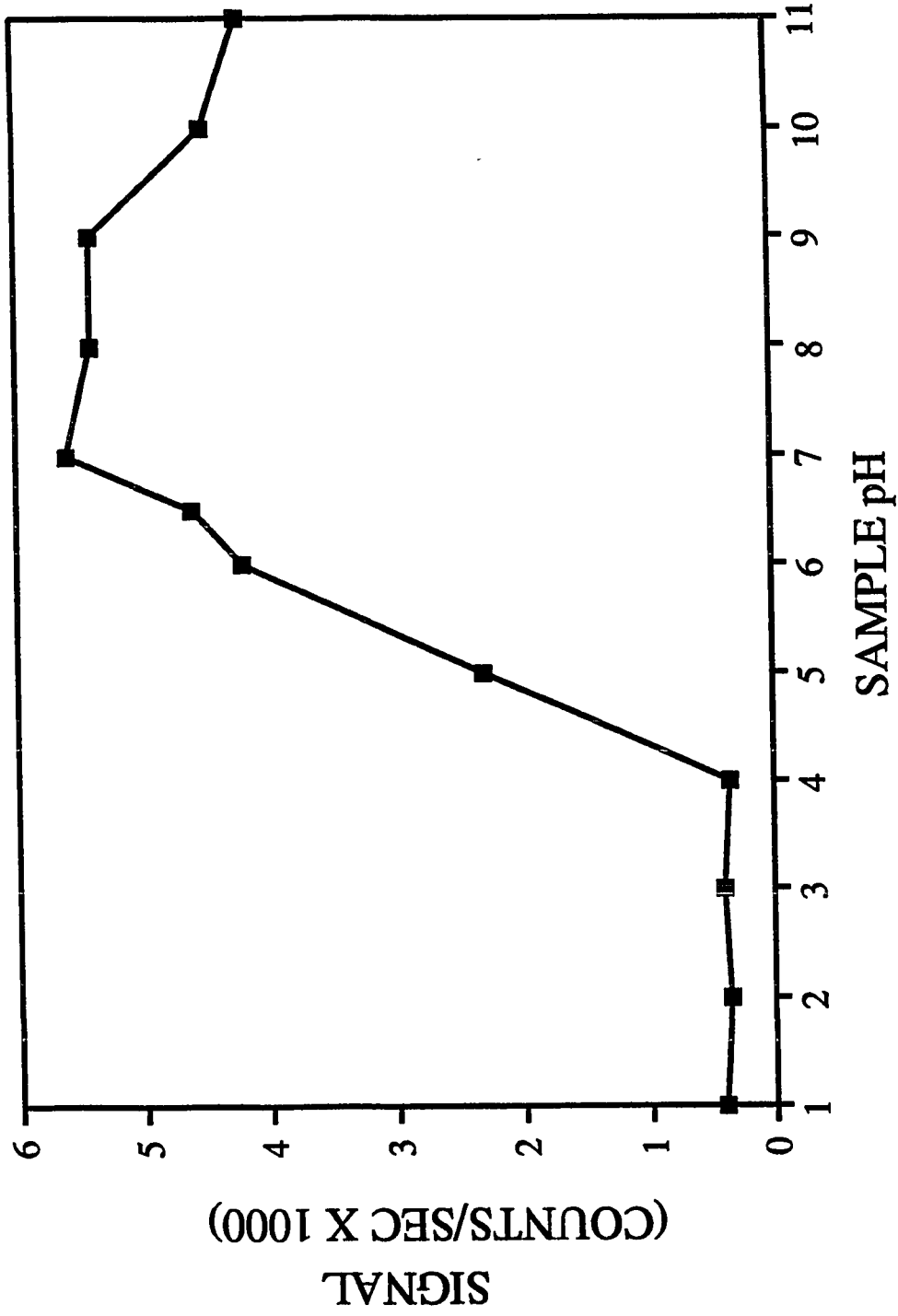
Figure 13. Effect of pH on the signal of a 5 nM Mn seawater sample. Seawater samples were analyzed at natural pH (~8) on board ship.
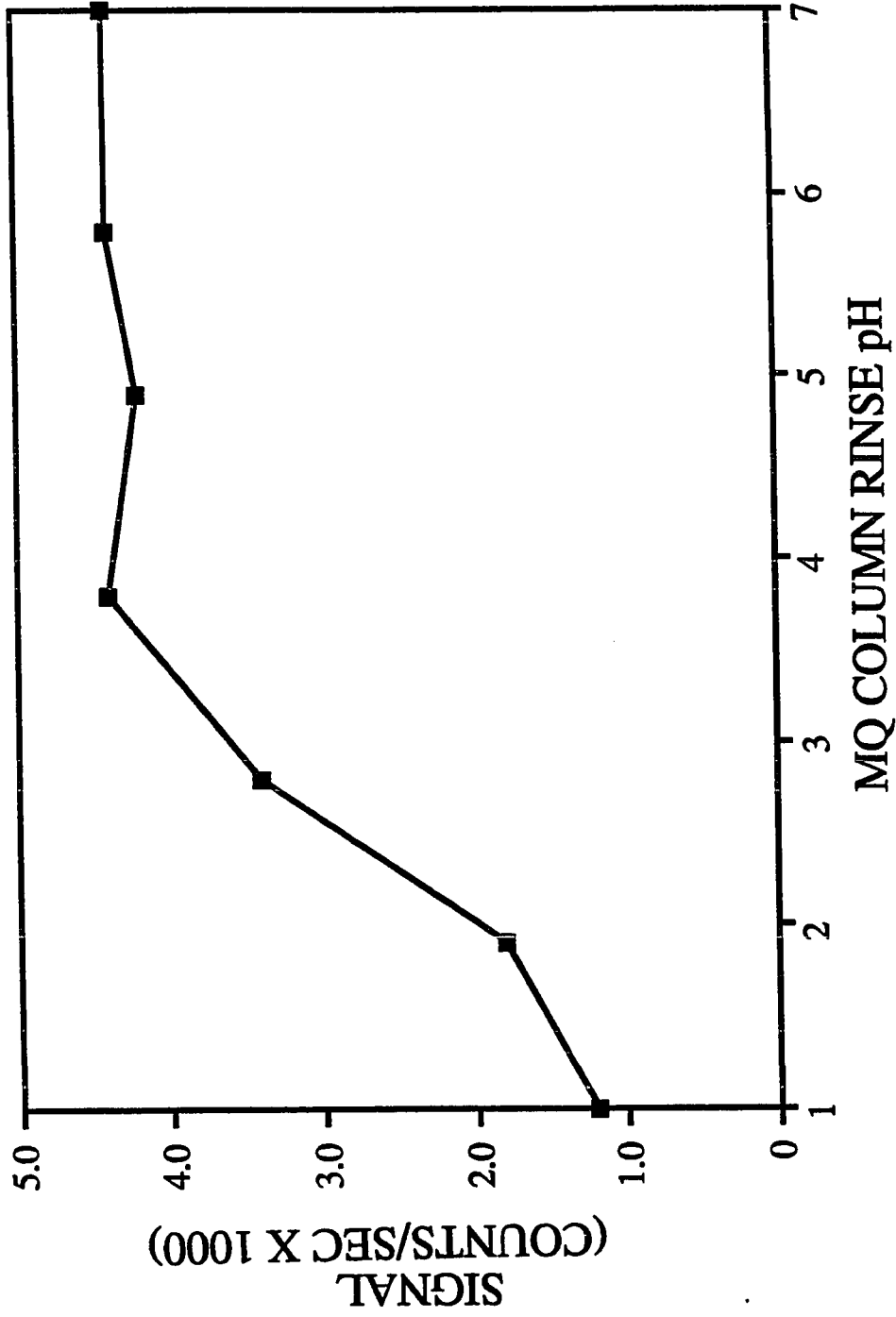
Figure 14. Effect of MQ rinse pH on signal of 50 nM seawater sample.
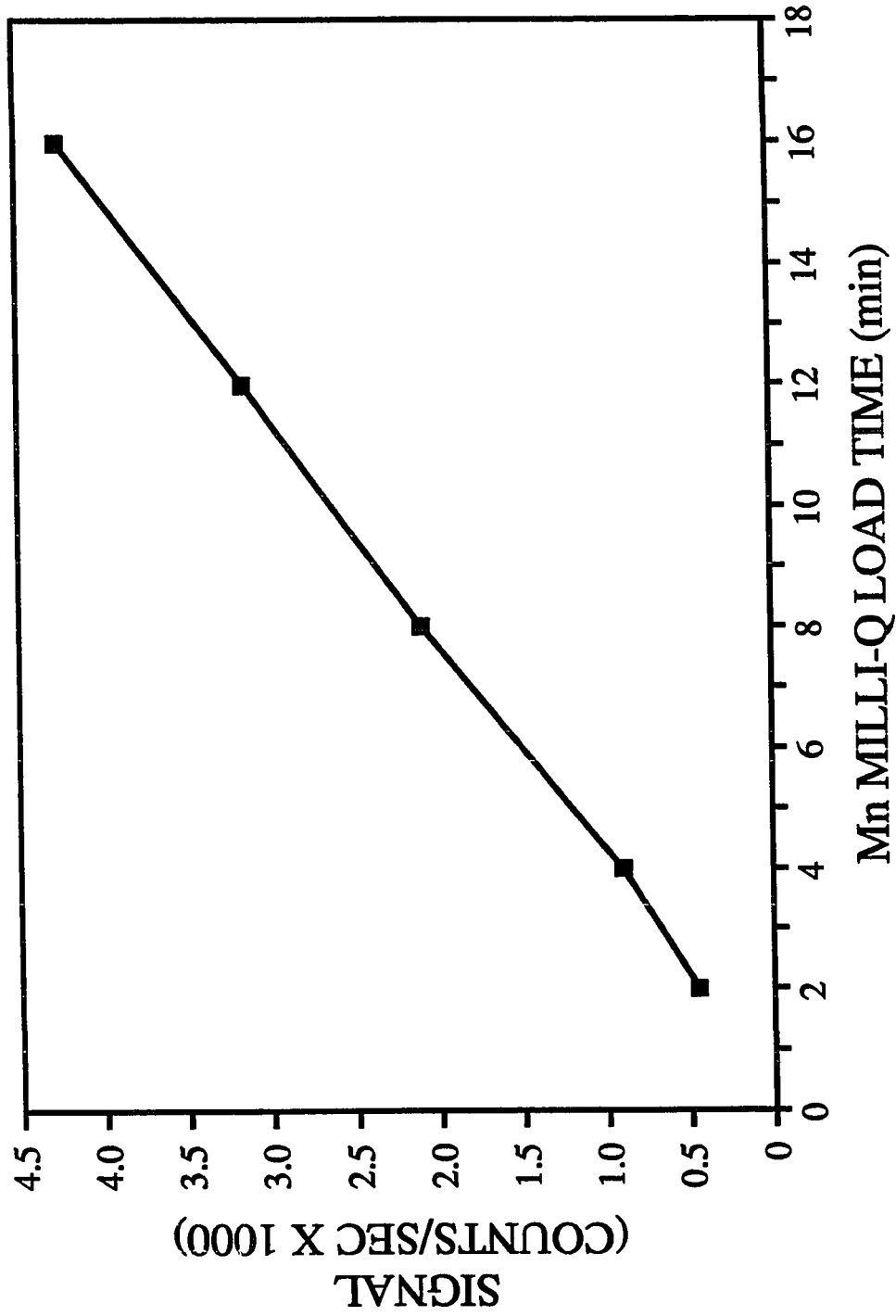MQ rinse pH was 6-7 during analysis.

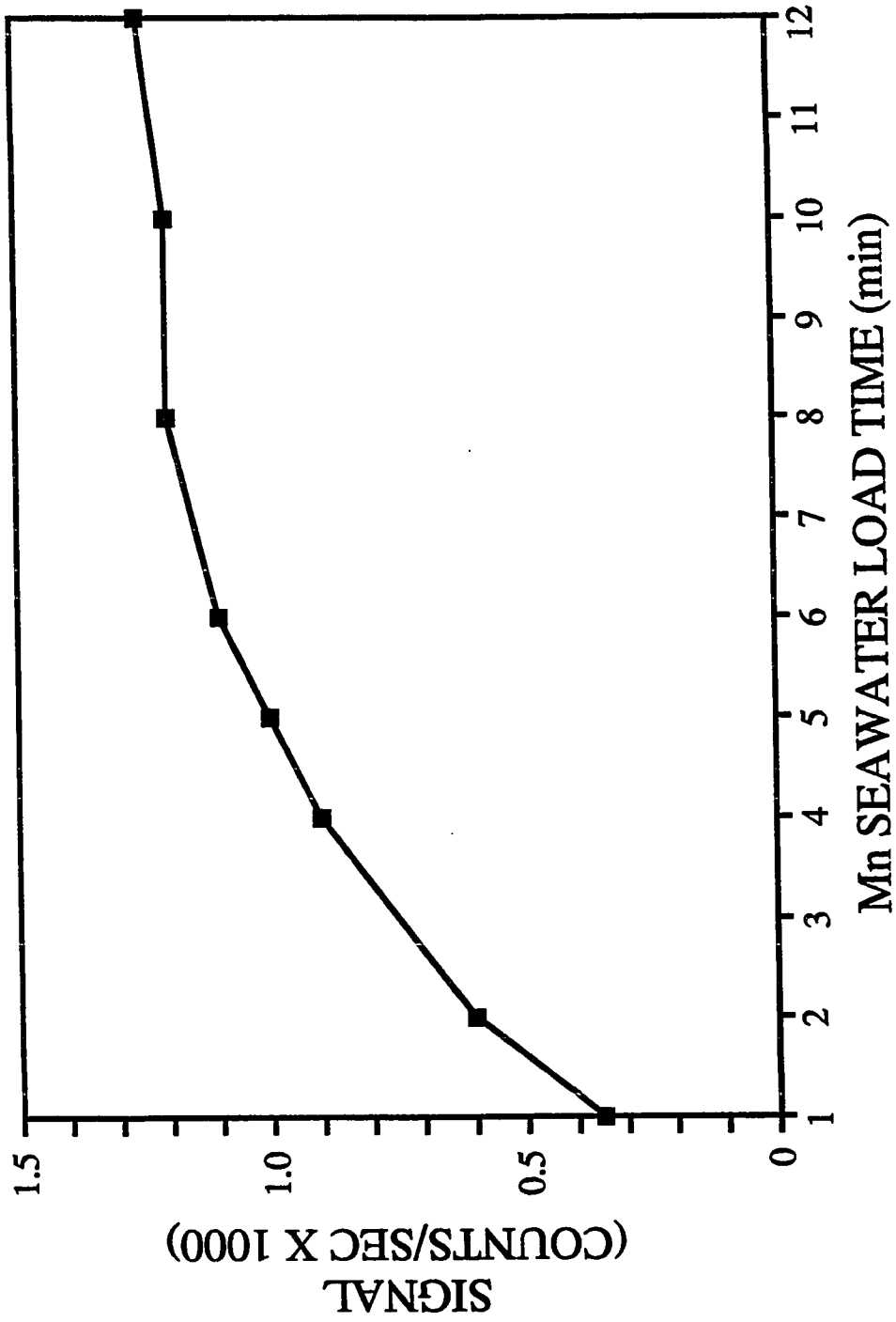Figure 15. Effect of load time on the signal of a 5 nM Mn MQ sample using a 1.0 cm 8-HQ column.

Figure 16. Effect of load time on the signal of a 2 nM seawater sample. A 4 minute load time was used during analysis.
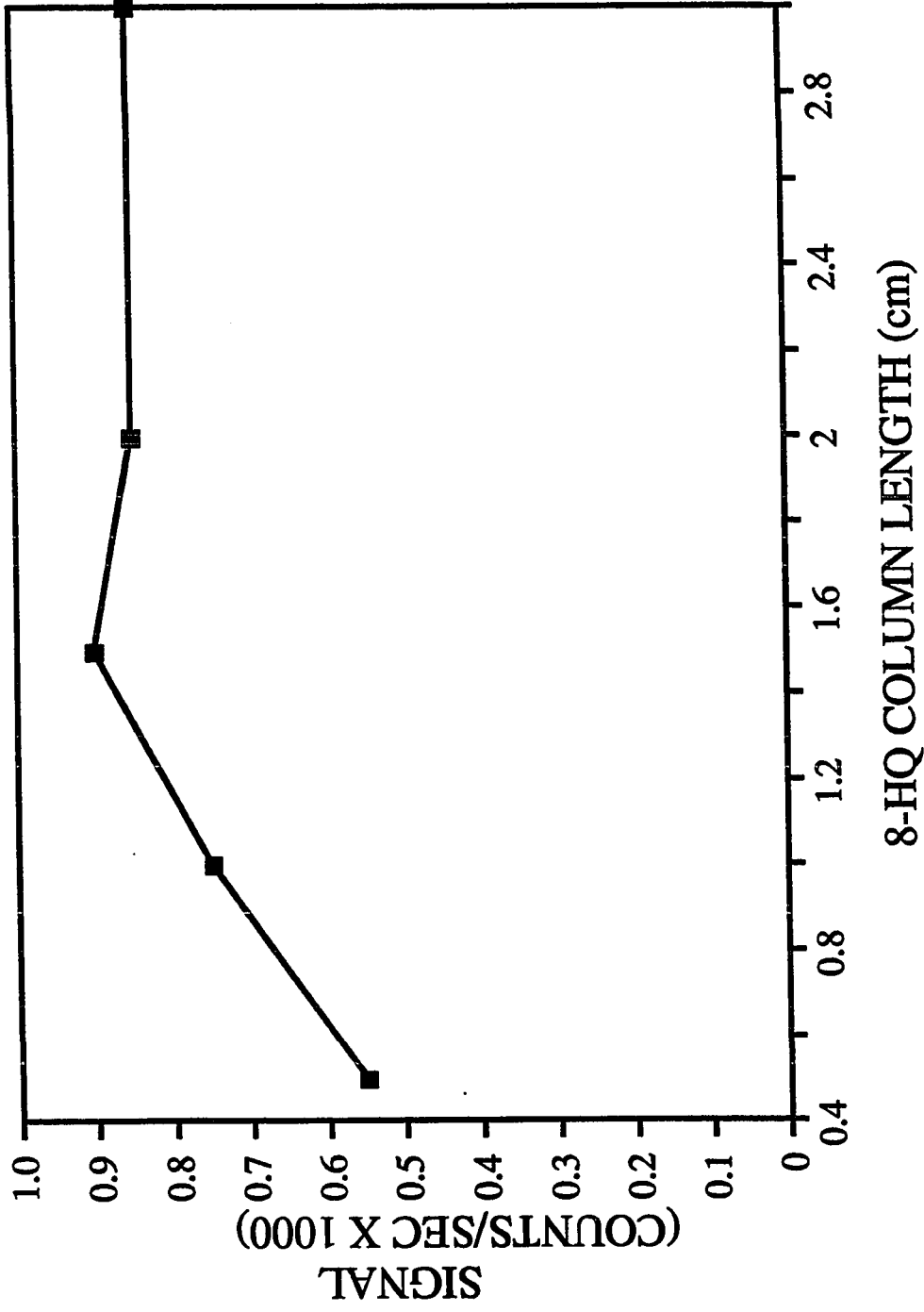
Figure 17. Effect of 8-HQ column length on the signal of a 2 nM Mn seawater sample. Both 1.0 and 1.5 cm columns were used during analysis.
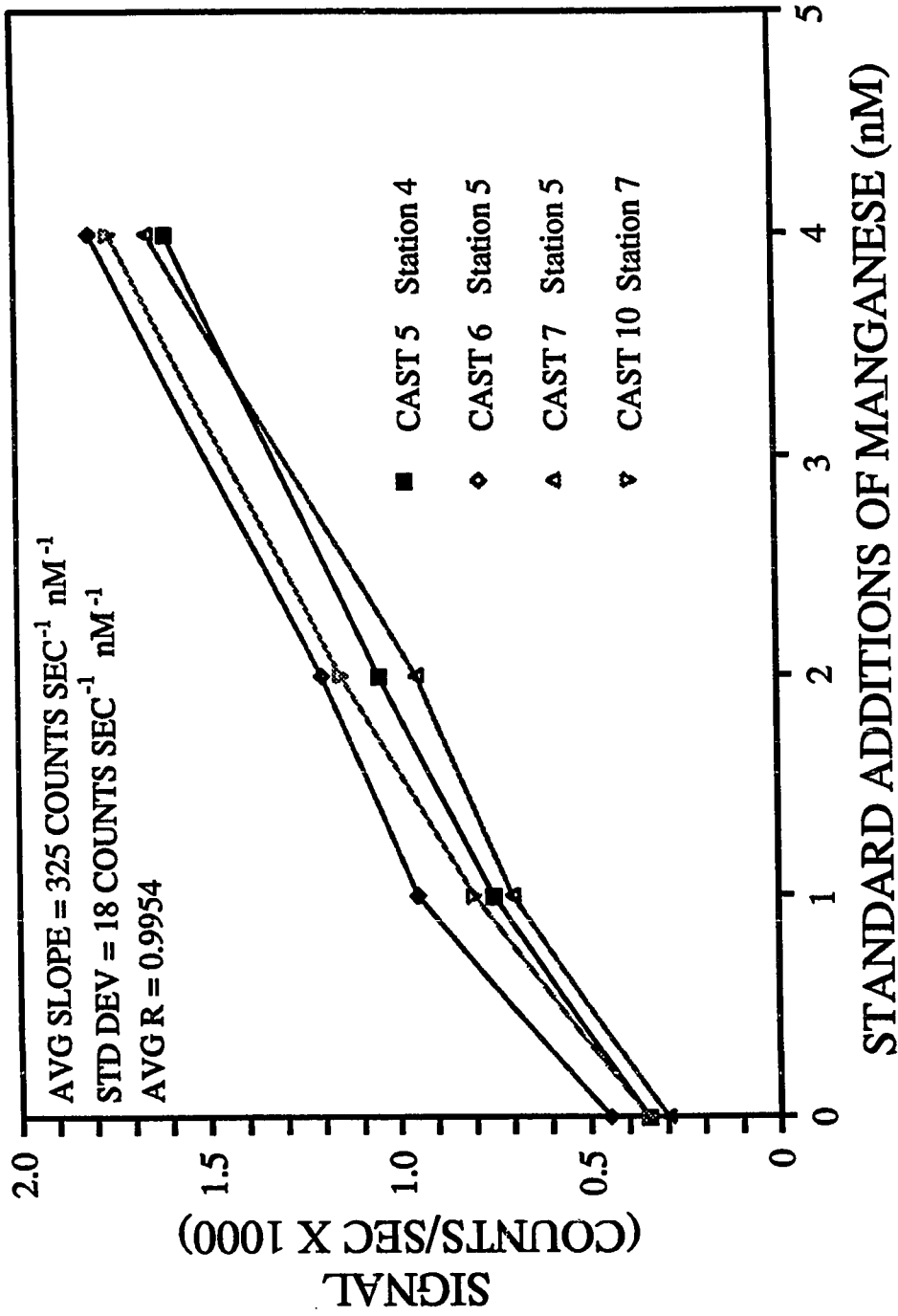
Figure 18. Mn standard addition curves for analyses run at sea on PS89 cruise, June 1-5, 1989.

Figure 19. Vertical profile of Mn analyzed at sea by
FIA-CL. GFAAS Mn data from a nearby station
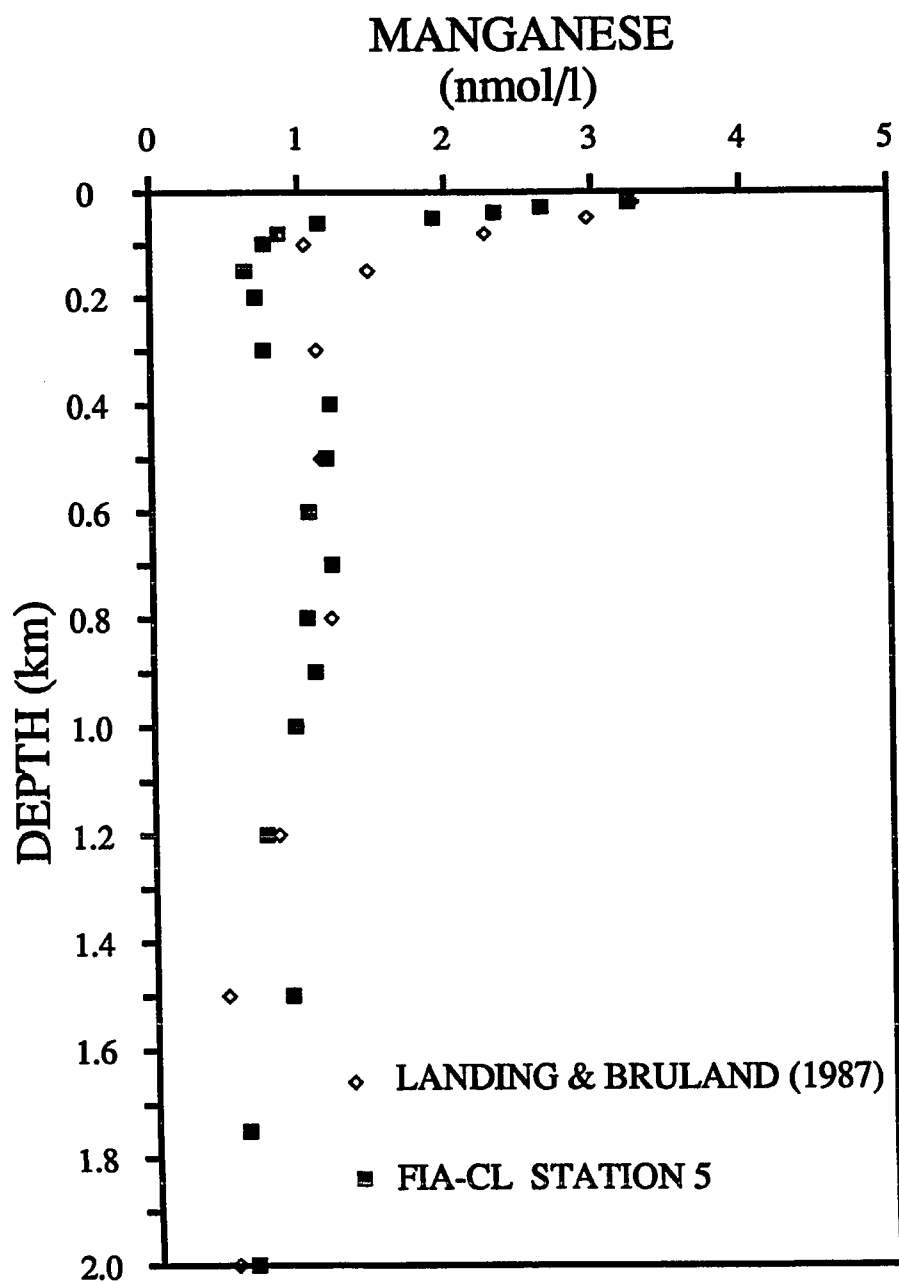is presented for comparison (1).

Figure 20. Vertical profile of Mn analyzed at sea by
FIA-CL. GFAAS Mn data from a nearby station
is presented for comparison (2).